

**Fluid-Structure Interaction of Multiphase Flow  
within a Pipe Bend**

by

**TAN CHEE HUAT**

**16072**

Dissertation submitted in partial fulfillment of the requirements for the

Bachelor of Engineering (Hons)

Mechanical

JANUARY 2015

UNIVERSITI TEKNOLOGI PETRONAS

Bandar Seri Iskandar

31750 Tronoh

Perak Darul Ridzuan

**CERTIFICATION OF APPROVAL**

**Fluid-Structure Interaction of Multiphase Flow  
within a Pipe Bend**

by

Tan Chee Huat

A project dissertation submitted to the  
Mechanical Engineering Programme  
Universiti Teknologi PETRONAS  
in partial fulfillment of the requirement for the  
BACHELOR OF ENGINEERING (Hons)  
MECHANICAL

Approved by,

---

(DR. TUAN MOHAMMAD YUSOFF SHAH B TUAN YA)

UNIVERSITI TEKNOLOGI PETRONAS

TRONOH, PERAK

May 2014

## **CERTIFICATION OF ORIGINALITY**

This is to certify that I am responsible for the work submitted in this project, that the original work is my own except as specified in the references and acknowledgements, and that the original work contained herein have not been undertaken or done by unspecified sources or persons.

---

TAN CHEE HUAT

## ABSTRACT

Multiphase flows are any fluid flow consisting of more than one phase or component, such as gas-liquid flow, liquid-liquid flow, liquid-solid flow or gas-liquid-solid-flow. It is commonly found in fluid transportation systems, particularly the hydrocarbons transportation systems in the oil and gas industry, accounted by simultaneous production of natural gases and crude oil. A significant response arising from flow-induced vibration could lead to potential fatigue damage or uncontrolled vibration when the excitation frequency matches the natural frequencies of the piping system, particularly in cases where oil brings dense sand particles or when slug flow develops in the flow-lines. This is therefore why the investigation of the effects of the oil-gas-water mixture on the structure of pipelines is important. Multiphase flow problems remain a challenge to the industry due to its complexity and unpredictability. This paper presents an analysis of fluid-structure interaction between a two-phase flow and a pipe bend to determine the resulting vibrations induced by the two-phase flow. Two pipe bend models with different upstream and downstream lengths of the bend are used for the analysis. Natural frequencies of the pipe bend structures are extracted and numerical simulations are performed using a CFD solver (ANSYS CFX module) and a FEA solver (ANSYS Mechanical module) coupled within ANSYS Workbench. Through Fast Fourier transforming the time domain results into frequency domain, the frequencies of vibrations are collected and compared with the natural frequencies to determine the corresponding level of risks.

## **ACKNOWLEDGEMENT**

My completion of Final Year Project will not be a success without the help and guidance from my supervisor and colleagues. Hereby, I would like to acknowledge my heartfelt gratitude to those I honor.

First of all, I would like to express my utmost gratitude to my direct supervisor, Dr. Dr. Tuan Mohammad Yusoff Shah, senior lecturer of Mechanical Engineering Department, Universiti Teknologi PETRONAS, for his valuable supervision, guidance, assistance and support throughout my project, especially on the technical aspects.

I would also like to thank Mr. Fazli Ahmat Jalaluddin, a staff at the UTP High Performance Computing Center (HPCC) whom had greatly helped me set up the access to HPC and guided me in submitting simulation jobs to be solved in the HPC facilities. I also wish to express my gratitude to my fellow colleagues, who were always there to provide valuable suggestions and comments on my works for further improvement.

Last but not least, I would like to thank my parents and my family members for their support. With their support, I managed to perform well and persevered through any obstacles faced during the project.

# TABLE OF CONTENTS

## LIST OF FIGURES AND TABLES

## ABSTRACT

## CHAPTER 1 INTRODUCTION

1.1 Background of Study	1
1.2 Problem Statement	2
1.3 Objectives	3
1.4 Scope of Study	3

## CHAPTER 2 LITERATURE REVIEW

2.1 Multiphase Flow	4
2.2 Pipe Bend	7
2.3 Fluid-Structure Interaction	8

## CHAPTER 3 METHODOLOGY

3.1 Governing Equations	11
3.1.1 Conservation of Mass	11
3.1.2 Conservation of Momentum	12
3.1.3 Conservation of Energy	12
3.2 Development of Pipe Bend Model	12
3.3 Development of Fluid Domain Model	13
3.4 Meshing of Pipe and Fluid Domain	14
3.5 Modal Analysis	15
3.6 Simulation Strategies	15
3.7 Screening Methodology	17
3.8 Project Process Flow Chart	18
3.9 Project Gantt Chart	19

<b>3.10 Tools Required</b>	<b>20</b>
<b>3.11 Concluding Remarks</b>	<b>20</b>
<b>CHAPTER 4 RESULTS AND DISCUSSION</b>	
<b>4.1 Natural Frequencies of Pipe Bend Models</b>	<b>21</b>
<b>4.2 Flow Patterns</b>	<b>21</b>
<b>4.3 Flow-Induced Vibration</b>	<b>23</b>
<b>4.3.1 Case 1A</b>	<b>24</b>
<b>4.3.2 Case 1B</b>	<b>27</b>
<b>4.3.3 Case 2A</b>	<b>30</b>
<b>4.3.4 Case 2B</b>	<b>33</b>
<b>4.3.5 Vibration Risk Assessment</b>	<b>36</b>
<b>CHAPTER 5 CONCLUSION &amp; RECOMMENDATIONS</b>	<b>37</b>
<b>REFERENCES</b>	<b>38</b>
<b>APPENDIX</b>	<b>40</b>

## LIST OF FIGURES

Figure 2.1: Flow Regimes in Horizontal Pipes

(Source:<https://build.openmodelica.org>)

Figure 2.2: Flow Pattern Map of Crude Oil and Natural Gas at 68 atm and 38°C in Horizontal Pipe. (Taitel & E, 1976)

Figure 2.3: Gas-Liquid flow Regime Map for Horizontal Pipe.

(Adapted from Shell DEP 31.22.05.11)

Figure 2.4: Streamlines of the secondary flow in the longitudinal section and the cross section of a 90° bend. (Azzi et. al, 2005)

Figure 2.5: Sources of excitation and interaction between liquid and piping.

(Adapted from D.C. Wiggert & A.S. Tijsseling (2001))

Figure 2.6: Simulation model of inlet pipe, elbow and the guide vane. (Adapted from Zhang et al., 2014)

Figure 2.7: PSD of Volume Fraction of Oil. (Chica, 2014)

Figure 3.1: Schematic drawing of Bend Model used.

Figure 3.2: Mesh of (a) Pipe Bend (b) Fluid Domain

Figure 3.3: FSI Simulation Approach (Source: ANSYS references)

Figure 3.4: FEA-CFD Coupling in ANSYS Workbench

Figure 3.5: Locations monitored (At bend)

Figure 3.6: Project Flow Chart

Figure 4.1: Water Volume Fraction Rendering (Case 1A)

Figure 4.2: Crude Oil Volume Fraction Rendering (Case 1B)

Figure 4.3: Water Volume Fraction Rendering (Case 2A)

Figure 4.4: Crude Oil Volume Fraction Rendering (Case 2B) Figure 4.5: Contour Plot of Displacement of the Pipe Bend.

Figure 4.6(a): Volume Fraction vs Time (Case 1A)

Figure 4.6(b): Volume Fraction PSD vs Frequency (Case 1A)



Figure 4.7(a): Von Mises Stress vs Time (Case 1A)

Figure 4.7(b): Von Mises Stress PSD vs Frequency (Case 1A)

Figure 4.8(a): Displacement vs Time (Case 1A)

Figure 4.8(b): Displacement PSD vs Frequency (Case 1A)

Figure 4.9(a): Volume Fraction vs Time (Case 1B)

Figure 4.9(b): Volume Fraction PSD vs Frequency (Case 1B)

Figure 4.10(a): Von Mises Stress vs Time (Case 1B)

Figure 4.10(b): Von Mises Stress PSD vs Frequency (Case 1B)

Figure 4.11(a): Displacement vs Time (Case 1B)

Figure 4.11(b): Displacement PSD vs Frequency (Case 1B)

Figure 4.12(a): Volume Fraction vs Time (Case 2A)

Figure 4.12(b): Volume Fraction PSD vs Frequency (Case 2A)

Figure 4.13(a): Von Mises Stress vs Time (Case 2A)

Figure 4.13(b): Von Mises Stress PSD vs Frequency (Case 2A)

Figure 4.14(a): Displacement vs Time (Case 2A)

Figure 4.14(b): Displacement PSD vs Frequency (Case 2A)

Figure 4.15(a): Volume Fraction vs Time (Case 2B)

Figure 4.15(b): Volume Fraction PSD vs Frequency (Case 2B)

Figure 4.16(a): Von Mises Stress vs Time (Case 2B)

Figure 4.16(b): Von Mises Stress PSD vs Frequency (Case 2B)

Figure 4.17(a): Displacement vs Time (Case 2B)

Figure 4.17(b): Displacement PSD vs Frequency (Case 2B)

## **LIST OF TABLES**

Table 2.1: Comparison of Single Phase and Multiphase

Table 2.2: Flow regimes of a Two-Phase Gas-Liquid Flow

Table 3.1: Pipe Bend Dimensions for Case 1 and Case 2

Table 3.2: Fluid Model parameters for Case A and Case B

Table 3.3: Mesh information of models

Table 3.4: Solver Settings used in ANSYS CFX.

Table 3.5: Properties measured at locations of interest

Table 3.6: Project Gantt chart

Table 4.1: First 8 modes of Pipe Structure

Table 4.2: Power Spectral Density Frequency of all Cases in Comparison with Natural Frequencies

# CHAPTER 1:

## INTRODUCTION

### 1.1 Project Background

Multiphase flow is the fluid flow consisting of more than one phase or component, such as immiscible fluids, or a solid component and a fluid. In upstream oil and gas industry, most if not all of the pipelines are handling multiphase flow as pressure and temperature drop significantly as hydrocarbons are lifted from the petroleum reservoir up to the platform for separation processes. The changes in temperature and pressure cause compositions of the fluid to change, i.e. split into liquid phase and gas phase. In reality, the compositions of the fluid are far more complex, accounting for waxes, hydrates, emulsions, solids, etc. In the context of this project, two types of two-phase fluid flow will be considered, namely water and vapor, and crude oil and gas.

Oil and gas industry is a multi-billion dollars industry. In Malaysia, oil and gas sector accounted for 20% of GDP (Gross Domestic Product) in 2012. In the upstream sector, flow assurance is of major importance because any incidents inhibiting or upsetting the flow of hydrocarbons are going to incur losses in millions of dollars to the oil company as well as impacting the economy. Fluid-structure interaction resulting in vibrations of the pipelines and flow behavior within the pipelines is one of the important keys to flow assurance issues, and it is even more crucial with multiphase flow. FSI is important and has received increased awareness over the past twenty years majorly due to safety and reliability concerns in plants, environmental issues and performance and safety in pipeline delivery systems. Numerous studies and researches have been conducted since the 1970s to understand and to quantify the mechanical interaction between unsteady flow in piping and the ensuing vibration of the piping structure. Many parameters dictate the FSI and its prediction method, for example, the properties of the fluid, flow behavior, piping geometry and so on. This project serves as an approach to FSI study and simulation of multiphase flow within a bend pipe.

## 1.2 Problem Statement

FSI is one of the important keys to flow assurance issues because excessive vibrations arising from FSI can cause dislodging of pipelines from the supporting mechanisms such as hangers and thrust blocks as well as an increased risk for pipe breakage. Whereas, perturbations in velocity and pressure of the flow could cause unsmooth flow and pose great problems to flow assurance. This problem is magnified in a multiphase flow, especially in a slug flow. To predict the resulting effects of multiphase flow FSI, the first thing needed is to model and predict the detailed behavior of the multiphase flow as well as the patterns that they exhibit. Then, the piping structure comes into play. In this project, it is within a pipe bend. Turning elements such as T-junctions and bends are the locations that are most subjected to flow-induced forces due to the changes of momentum of the fluids. The effects of fluid flow on the adjacent structure or body, i.e. piping structure, vary with the fluid flow characteristics, including its compositions, density, viscosity, volatility and turbulence.

Multiphase flow often presents a far more complex and unpredictable flow behavior than single phase flow. Consequently, the FSI arising from multiphase flow is difficult to predict. One of the reasons is because the density and other properties of the fluid are very difficult to estimate as different phase and components exist. Simulation often requires very high computing power, not to mention multiphase flow FSI simulation where the model can be very complex. Fortunately, computational methods have evolved over the past decades witnessing the birth of high performance computers and powerful computing software such as ANSYS. These breakthroughs have given new breath to FSI modeling and prediction. However so, even in simplified simulation where only two-phase - crude oil (liquid) and gas phase, the density, compositions, and other properties of the fluid vary from each reservoir depending on its nature, temperature and pressure, age of reservoir and composition. Thus, there are many variables that have to be taken into consideration and there are variables that have to be assumed during multiphase flow FSI simulation. One of the important criteria is to make correct and accurate assumptions.

### **1.3 Objectives**

For this project, numerical simulation of liquid-liquid flow is conducted and aimed:

- a) To determine the resulting levels of flow-induced vibration arising from multiphase flow within a horizontal pipe bend.
- b) To determine the risk of vibrations induced by a two-phase flow.

### **1.4 Scope of Study**

Due to the high difficulty and complexity in modeling and simulating multiphase flow, the project will first cover single phase flow FSI simulation and then move on to multiphase flow FSI, where two stages of simulations will be done, namely for water & air and for crude oil & gas. This is a measure for comparative study as well as an approach of familiarization with the software and simulation procedures.

The scope of study includes but not limited to the following:

- Study of Computational Fluid Dynamics software (ANSYS CFX).
- Investigation of properties of crude oil and natural gases.
- Investigation of multiphase flow patterns and its parameters.
- Simulation of multiphase flow FSI for water and air
- Simulation of multiphase flow FSI for crude oil and gas.

## CHAPTER 2: LITERATURE REVIEW

### 2.1 Multiphase Flow

Bakker (2006) defines multiphase flow as a simultaneous flow of materials with distinctive states or phases, such as gas, liquid or solid. It can also be a flow of materials in the same state or phase but with different chemical properties, such as oil-droplets in water. According to Bakker (2006) also, there are several regimes of multiphase flow. An example distinguishing single phase and multiphase is shown in Table 2.1. In the context of this thesis, the main concern is on two-phase gas-liquid flow.

Multiphase flow modeling is a very complex work. Not only there are limitations in time, computing power is also a key to whether or not a multiphase flow can be modeled accurately. Some models have been developed that are suitable for different multiphase flow applications and exhibit different levels of accuracy and applications; they are Eulerian-Lagrangian, Eulerian-Eulerian, Volume of Fluid, etc.

Table 2.1: Comparison of Single Phase and Multiphase

	Single component	Multi-component
Single Phase	Water Pure Nitrogen	Air H <sub>2</sub> O + Oil Emulsions
Multiphase	Steam bubble in H <sub>2</sub> O Ice Slurry	Coal Particles in Air Sand Particles in H <sub>2</sub> O

Similar to single-phase flow, a multiphase flow follows the three main conservation principles, namely the conservation of mass, momentum and energy. These principles apply for each phase in a multiphase flow. Therefore, there would be at least two sets of each of the conservation laws in multiphase flow. Simplifications were made by some pioneers such as Bratland (2010) for multiphase flow.

There are several regimes of two-phase gas-liquid flow. They are illustrated in Figure 2.1 and summarized in Table 2.1. A flow regime describes the geometrical distribution

of the phases. The regime in which the fluid flows also significantly affects phase distribution, velocity distribution and so on (Stenmark, 2013).

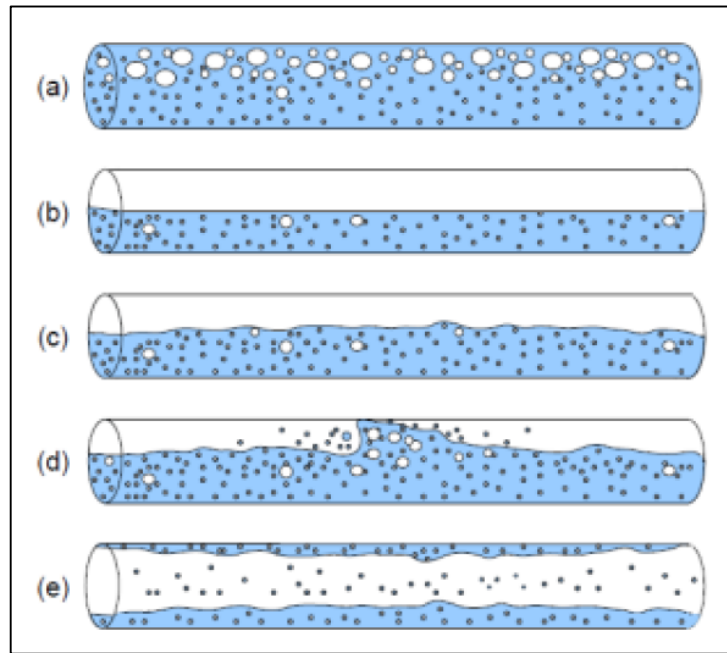


Figure 2.1: Flow Regimes in Horizontal Pipes (Source: <https://build.openmodelica.org>)

Table 2.2: Flow regimes of a Two-Phase Gas-Liquid Flow

Multiphase Flow Regime	Characteristics
Bubbly flow (a)	Discrete gaseous bubbles in a continuous liquid.
Stratified and free-surface flow (b)	Immiscible fluids separated by a clearly-defined interface.
Wavy flow (c)	Superficial velocity of gas increases and waves starts forming at the interface boundary due to surface tension.
Slug flow (d)	Discontinuous elongated bubbles separated by chunks of liquids that blocks the pipe.
Annular flow (e)	Continuous liquid along walls, gas in core. Occurs when superficial velocity of gas is very high in comparison to the liquid.

In order to simulate the flow in the desired flow pattern, a flow regime map is to be referred, such as the Taitel-Dukler flow regime map as shown in Figure 2.1. The Taitel-

Dukler flow regime map is based on the superficial velocities of the phases. Another flow-regime map as adapted by Shell Design and Engineering Practice (DEP) Standard 31.22.05.11 is the gas-liquid two-phase flow regime map (Figure 2.3) based on the Froude numbers of each phase.

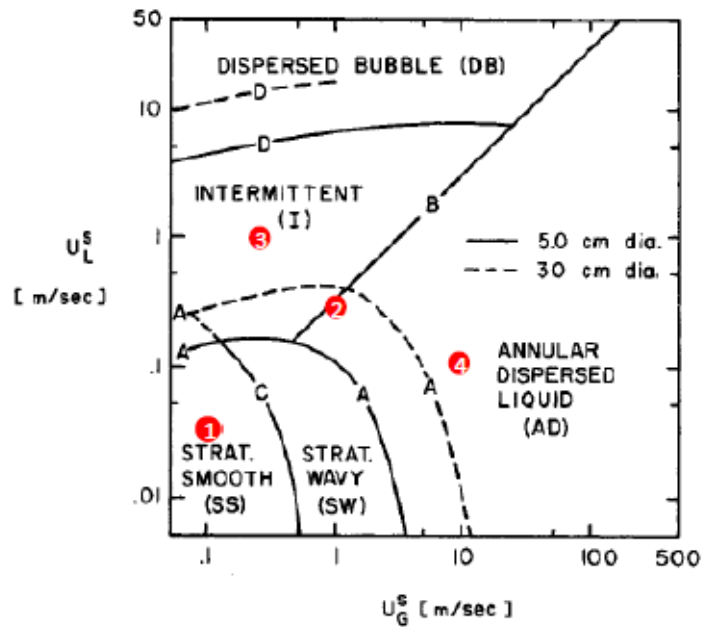


Figure 2.2: Flow Pattern Map of Crude Oil and Natural Gas at 68 atm and 38°C in Horizontal Pipe. (Taitel & E, 1976)

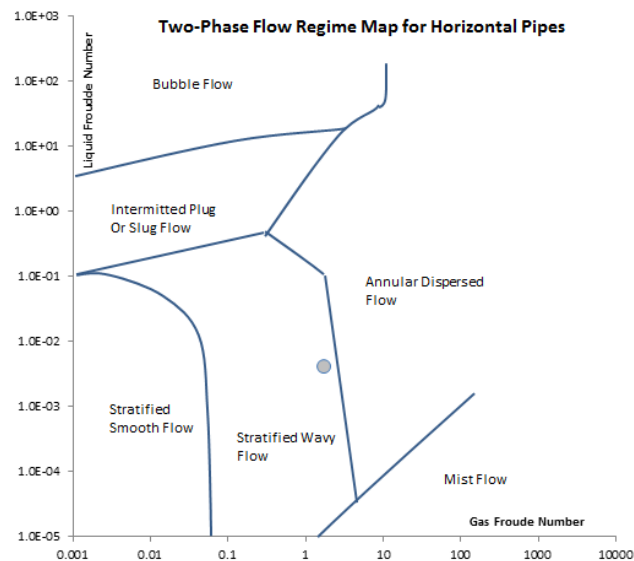


Figure 2.3: Gas-Liquid flow Regime Map for Horizontal Pipe. (Adapted from Shell DEP 31.22.05.11)

Chica (2014) developed a screening methodology for assessing flow-induced vibration (FIV) due to multiphase flows using a combination of STAR-CCM+ tool and FEA



code ABAQUS. Comparisons were made between two-phase, three-phase and four-phase flows. Horgue et al. (2012) researched on the suitable parameterization to simulate slug flows using Volume-of-Fluid method. Suitable parameterization is important for accuracy and computation speed. Less compressive schemes is preferred instead of the most compressive scheme because it allows for coarser meshes while maintaining fine accuracy and avoiding numerical errors. Wiggert & Tijsseling (2001) discussed that the source of FSI excitation can be due to swift changes in flow and pressure or due to mechanical action of the piping. Vallee et al. (2007) successfully simulated two-phase slug flow using ANSYS CFX and validated his results with experiment. The results shown that CFX calculation were very accurate in predicting flow pattern formed by two-phase flow.

Brennen (2005) argues that unlike single-phase flow where an entrance length of 30 to 50 diameters is required for fully developed turbulent flow, multiphase flow is complex and the corresponding entrance lengths are less well established. He emphasizes that a flow regime map does not always accurately predict a certain flow pattern for a given fluids with given flow rates.

## **2.2 Pipe Bend**

According to Thorley (2004), the design of pipeline systems has to go through a series of stages, those are: initial conception, feasibility studies, functional design, optimization and risk assessment. Quick changes in the flow rates and direction of liquid or two-phase piping systems can cause pressure transients that generate pressure pulses and transient forces in the piping system. The magnitudes of these pressure pulses and force transients are often difficult to predict and quantify. In designing pipe bends, there are a certain standards that have to be followed, especially for the multi-billion dollar oil and gas application.

According to Mazumder Q. H., (2012), the curvature of a pipe bend causes a centrifugal force which is directed from the momentary center of curvature toward the outer wall. The combination of the presence of boundary layer at the wall due to the fluid adhesion to the wall and the centrifugal force produce a secondary flow as illustrated in Figure 2.4. This secondary flow is superimposed to the mainstream along the tube axis. As a result, a helical shape streamline is flowing through the bend.

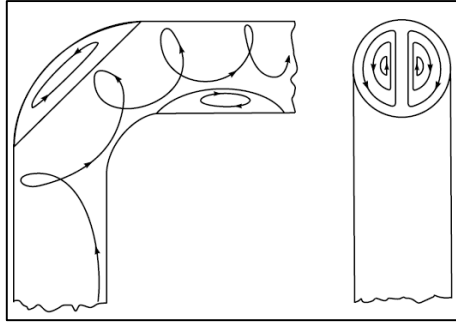


Figure 2.4: Streamlines of the secondary flow in the longitudinal section and the cross section of a 90° bend. (Azzi et. al, 2005)

In a study conducted by Sekoda K. et al., (1969), it was found that in a two-phase bend, the pressure drop is dependent on the  $r/D$  ratio but is independent of pipe diameters. Besides  $r/D$  ratio, the equivalent length to diameter ratio,  $L_e/D$  is also of importance. Mazumder Q. H. (2012) states that, for a fully-developed flow, a  $L_e/D$  ratio of 100 to 150 is required. Whereas for  $r/D$  ratio, the standard values for a 90° pipe bend are  $4D$  and  $5D$  for bends and  $1.5D$  for elbow according to PETRONAS Technical Standards 31.38.01.11. In an experimental investigation regarding the pressure drop of turbulent across a 90° elbow conducted by Crawford et al. (2007), it was found discovered that the flow displayed axial symmetry characteristics and the normal stress distributions of the turbulent flows were more uniform than fully-developed pipe flows. It was also inferred that the bend curvature accelerated the swirl decay in a pipe flow.

### 2.3 Fluid-Structure Interaction (FSI)

Fluid-structure interaction (FSI) is the study of interaction between an internal or surrounding fluid flow and a movable or deformable structure that contains or in contact with the fluid flow, such as piping. FSI in piping systems is generally made up of the conveyance of momentum and forces between piping and the contained fluid during unsteady flow. According to Wiggert & Tijsseling (2001), the source of FSI excitation can be due to swift changes in flow and pressure or due to mechanical action of the piping. The result of the interaction is a manifestation of pipe vibration, disturbance in velocity and pressure of the fluid.

There are three identified coupling mechanisms (Wiggert & Tijsseling, 2001):

- Poisson Coupling – Associated with the axial stress perturbations translated by virtue of Poisson ratio coefficient from the circumferential or hoop stress perturbations caused by liquid pressure transients. The axial stress and strain propagate as waves in the piping wall at a speed near to that of a sound's in solid beams.
- Friction Coupling – Usually insignificant compared to the other two mechanisms, friction coupling is produced by the transient liquid shear stresses acting on the pipe wall.
- Junction Coupling – Being the most significant coupling mechanism, junction coupling is produced by reactions due to unbalanced pressure forces and fluctuations in liquid momentum at discrete locations, i.e. bends, valves, orifices and tees.

It should be noted that other than those related to fluid motion, the source of excitation may also come from the structural side, such as those illustrated in Figure 2.5.

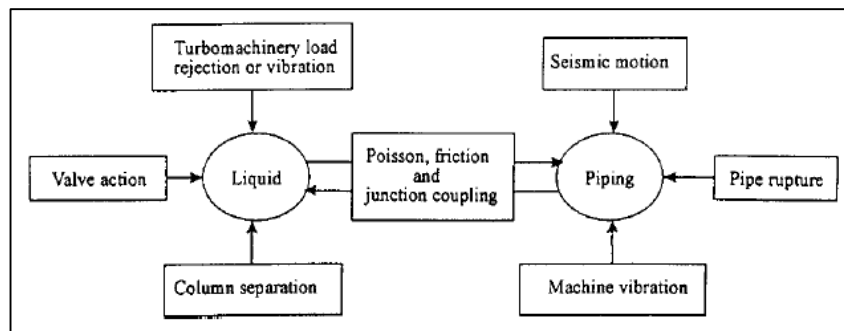


Figure 2.5: Sources of excitation and interaction between liquid and piping.  
(Adapted from D.C. Wiggert & A.S. Tijsseling (2001))

Zhang et al. (2014) performed a FSI simulation using water in a 90° piping elbow with a radius ratio of 1.5 with the Large Eddy Simulation (LES) method. The study determined the structural vibration and fluid-borne noise induced by turbulent flow. The configuration of their fluid model is illustrated in Figure 2.6.

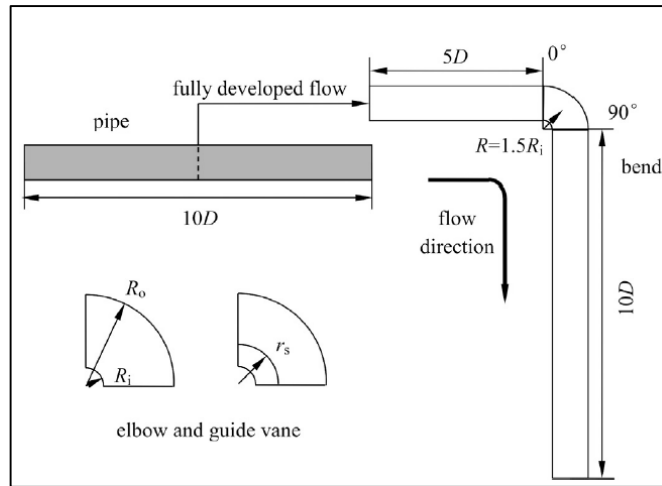


Figure 2.6: Simulation model of inlet pipe, elbow and the guide vane. (Adapted from Zhang et al., 2014)

Chica (2014) performed FSI simulation on an M-shaped jumper using two-phase and three-phase flow to determine the flow-induced vibration. He also proposed a screening methodology of determining the flow-induced vibration levels from multiphase flow. He monitored the fluctuations of volume fraction of liquids, pressure, stresses and displacement at points of interest such as bends, and translate the response into frequency domain (power spectral density vs frequency) to identify the dominant frequency, as illustrated in Figure 2.7. According to Energy Institute (2008), it is recommended that the excitation frequency does not fall within  $\pm 20\%$  of the natural frequency of the structure.

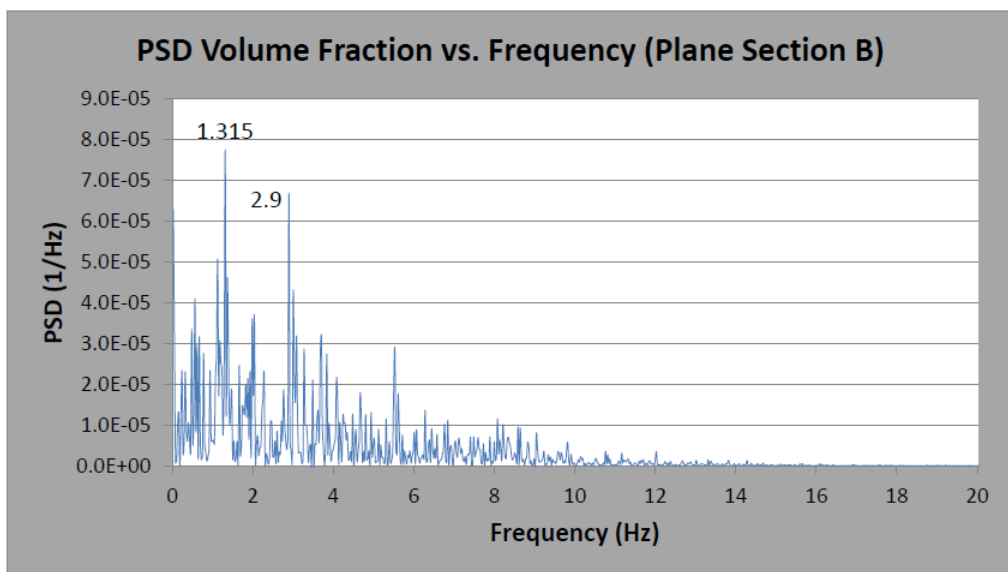


Figure 2.7: PSD of Volume Fraction of Oil. (Chica, 2014)

## CHAPTER 3:

### METHODOLOGY

Throughout the project, comprehensive preliminary studies into previous researches has been carried out. This research is started with the development of a pipe bend. As discussed in Chapter 2, pipe bends require certain standards and requirements, and the model used is in comply with it to validate for the practical cases. Based on the respective scope of study, numerical simulation is set up and performed on the pipe bend model to generate the results. The results obtained is firstly validated with experimental data, and then being analyzed to study the two-phase separation efficiency to meet the pre-stated objectives.

#### 3.1 Governing Equations

The governing equations for Eulerian multiphase model can be summarized as follows in Eqn. 3.1, Eqn. 3.2 and Eqn. 3.3

##### 3.1.1 Conservation of Mass

$$\frac{\delta(\alpha_k \rho_k)}{\delta t} + \frac{\delta}{\delta x}(\alpha_k \rho_k v_k) = \Gamma_{ki} + \Gamma_{kw} \quad (3.1)$$

The first, second, third and fourth term of the equation refers to the accumulated mass inside the pipe, total mass flow into the pipe, the mass flow from other phases and total mass flow from other external sources respectively.

##### 3.1.2 Conservation of Momentum

$$\sum_{k=1}^N R_{ki} + S_{ki} + v_k \Gamma_{ki} = 0 \quad (3.2)$$

In addition to the Newton's second law, additional forces are considered to account for the phase-to-phase interactions. These are the forces responsible to change the flow pattern throughout the flow path.  $R_{ki}$  represents the friction force from other phases,  $S_{ki}$  is the force due to surface tension from other phases, and  $v_k \Gamma_{ki}$  is the mass transfer or momentum exchange.

### 3.1.3 Conservation of Energy

Considering all the internal and external energy sources acting on the phases, the equation is given as:

$$\frac{\delta}{\delta t}(\alpha_k E_k) = - \frac{\delta}{\delta x}[\alpha_k v_k (E_k + p_k)] + q_{ki} + q_{kw} + w_{ki} + w_{kw} + \Gamma_{ki} h_{ki} + \Gamma_{kw} h_{kw} \quad (3.3)$$

The first term represents the internal energy,  $q$  is the specific heat,  $w$  is the specific work,  $\Gamma$  is the specific mass flow term, and  $h$  refers to the specific enthalpy. The subscript “i” and “w” refer to the energy coming from other phases and from outside to a phase  $k$  respectively.

### 3.2 Development of Pipe Bend Model.

The pipe bend model is developed according to the schematic diagram shown in Figure 3.1. The bend model has a radius curvature  $R_c$ , a length of  $L_{in}$  upstream of the bend and a length of  $L_{out}$  downstream of the bend. The developed model is meshed and solved simultaneously with the CFD solver (ANSYS CFX). The  $L_{in}$  and  $L_{out}$  are varied to allow for possible slug to develop if any. The pipe is to be modelled as horizontal since the fluid flow is also horizontal.

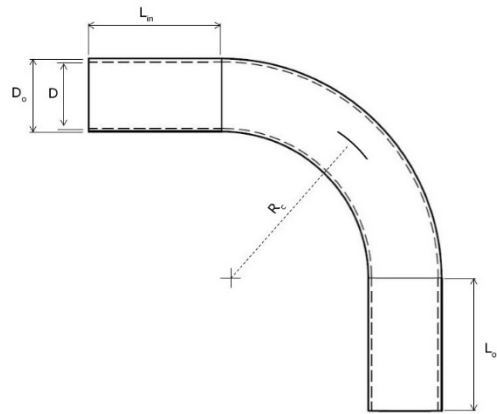


Figure 3.1: Schematic drawing of Bend Model used.

Two cases for the pipe bends are used and the dimensions for each case is as shown in Table 3.1.

Table 3.1: Pipe Bend Dimensions for Case 1 and Case 2

	Case 1	Case 2
$L_{in}$	0.2m	1.0m
$L_{out}$	0.2m	0.5m
D	0.05m	
$D_o$	0.055m	
$R_c$	0.25m	
R/D	5	

### 3.3 Development of Fluid Domain Model

The fluid model is essentially the hollow inner part of the pipe bend model. Two cases of two-phase flow were studied, one using water & air and another using crude oil & natural gas. The flow is horizontal and is initialized as stratified flow with initial volume fraction of 0.5 for each phase. Table 3.2 lists the parameters of flow in each case.

Table 3.2: Fluid Model parameters for Case A and Case B

	Case A (Water & Air)	Case B (Crude Oil & Gas)
$\dot{m}_{liquid}$	7000 kg/hr	4608 kg/hr
$\dot{m}_{gas}$	50 kg/hr	180 kg/hr
$\rho_L$	997 kg/m <sup>3</sup>	650 kg/m <sup>3</sup>
$\rho_G$	1.185 kg/m <sup>3</sup>	50 kg/m <sup>3</sup>
P	1 atm	68 atm
T	25°C	38°C

The parameters for Case A is based on Froude number of each phase in accordance to Shell DEP 31.22.05.11 standard whereas the parameters for Case B is based on the Taitel-Dukler regime map (Figure 2.2). The densities are taken at the respective pressure and temperature of the fluid. The superficial velocities and Froude numbers are calculated based on equations 3.4 – 3.7.

Liquid Superficial Velocity:

$$U_{SL} = \frac{Q_L}{A} \quad (3.4)$$

Gas Superficial Velocity:

$$U_{SG} = \frac{Q_G}{A} \quad (3.5)$$

Liquid Froude Number:

$$Fr_L = U_{SL} \sqrt{\frac{\rho_L}{(\rho_L - \rho_G)gD}} \quad (3.6)$$

Gas Froude Number:

$$Fr_G = U_{SG} \sqrt{\frac{\rho_G}{(\rho_L - \rho_G)gD}} \quad (3.7)$$

### 3.4 Meshing of Pipe and Fluid Domain

The meshing of the pipe (solid domain) and the fluid domain are meshed separately each under ANSYS Transient Structural Module and ANSYS CFX module. Both domains are meshed using sweep method (Fig 7) with mixed Quad/Tri elements and “Advanced Sizing Function” turned on at curvature.

Coarser mesh is used as a compromise to limited computational resources and time. Table 3 lists the mesh information for each domain for Case 1 and Case 2. The meshes are of good quality with aspect ratio well below the recommended maximum aspect ratio of 18-20 by ANSYS documentation. Figure 3.2 and Table 3.3 illustrate the mesh quality of both domains.

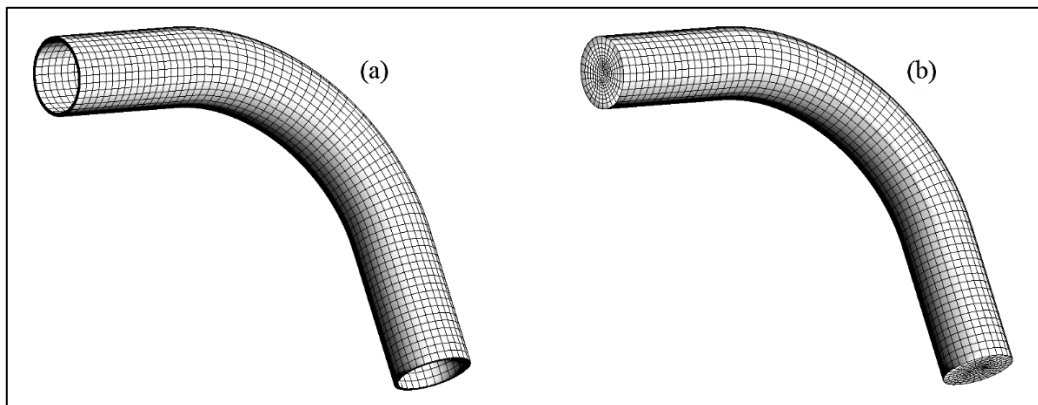


Figure 3.2: Mesh of (a) Pipe Bend (b) Fluid Domain



Table 3.3: Mesh information of models

	Case 1		Case 2	
	FEA	CFD	FEA	CFD
No. of Elements	14122	65678	16926	68832
No. of Nodes	2112	15510	4200	17552
Max Aspect Ratio (<100)	6.22	13.24	12.38	12.67
Max Skewness (<1)	0.80	0.53	0.85	0.57

### 3.5 Modal Analysis

Modal analysis is performed in ANSYS Workbench to extract the natural frequencies of the pipe structure under several constraints. Forced vibrations if excited at the same frequency as the natural frequency, resonance will occur and significant vibrations can happen. The natural frequencies and its respective mode shapes are derived according to Eqn. 3.8.

$$[M][\ddot{U}] + [K][U] = 0 \quad (3.8)$$

Where, M is the mass matrix,  $\ddot{U}$  is the acceleration and K is the stiffness matrix.

### 3.6 Simulation Strategies

The FSI simulation is divided into two domains, namely the FEA domain and CFD domain which are coupled together and solved successively, as illustrated in Figure 3.3 and Figure 3.4. The coupling approach is done in ANSYS Workbench between the CFD solver ANSYS CFX and the FEA solver ANSYS Mechanical. The settings used for the solver is as shown in Table 3.4. A total of four cases were analyzed based on Table 3.1 and Table 3.3. Namely, Case 1A, Case 1B, Case 2A and Case 2B.

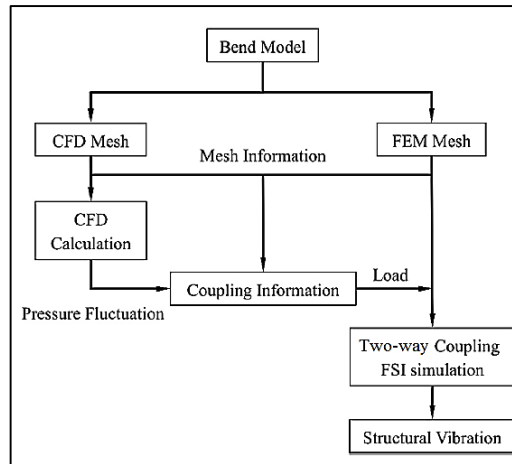


Figure 3.3: FSI Simulation Approach (Source: ANSYS references)

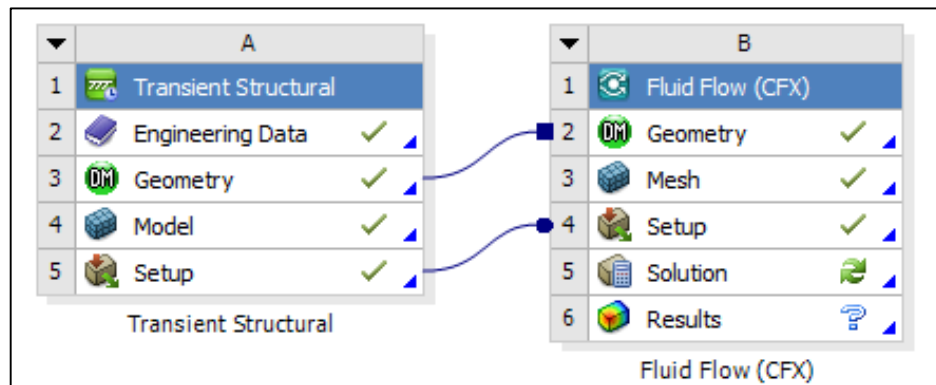


Figure 3.4: FEA-CFD Coupling in ANSYS Workbench

Table 3.4: Solver Settings used in ANSYS CFX.

Solver Settings	Settings Used
Multiphase Model	Free Surface
Turbulence Model	k- $\omega$ Shear Stress Transport (SST)
Wall	No Slip Wall
Advection Scheme	Upwind
Transient Scheme	Second Order Backward Euler
Convergence Criteria	RMS 1E-4
Time Step	0.01 seconds
Total Time	10 seconds
Near-Wall Treatment (Y+)	30 layers total thickness

### 3.7 Screening Methodology

A modal analysis is first performed to extract the natural frequencies of the pipe bend models for each of Case 1 and Case 2 using the Modal Analysis module available in ANSYS Workbench.

Subsequently, the FSI simulations are performed to determine the flow-induced vibration levels and are compared to the natural frequencies extracted. Three locations of interests in the bend are monitored in the simulations (Fig 3.5).

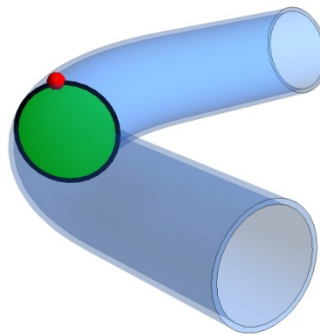


Figure 3.5: Locations monitored (At bend)

The first stage of screening is by using the fluctuations in volume fractions of liquid in the fluid domain cross-section plane at the bend (colored in green). The results are then verified with the FSI results in the solid domain's locations of interests, namely the point colored in red (monitors displacement) and the cross-section plane colored in black (monitors Von Mises Stress). The screening method is in accordance to the screening methodology proposed by Chica (2014).

Table 3.5: Properties measured at locations of interest

Location	Properties monitored
Plane in Green	Volume Fraction of Liquid
Plane in Black	Von Mises Stress of Pipe
Red Dot	Displacement of Pipe

### 3.8 Project Process Flow Chart

The project is conducted methodically based on the project process flow chart as shown in Figure 3.6.

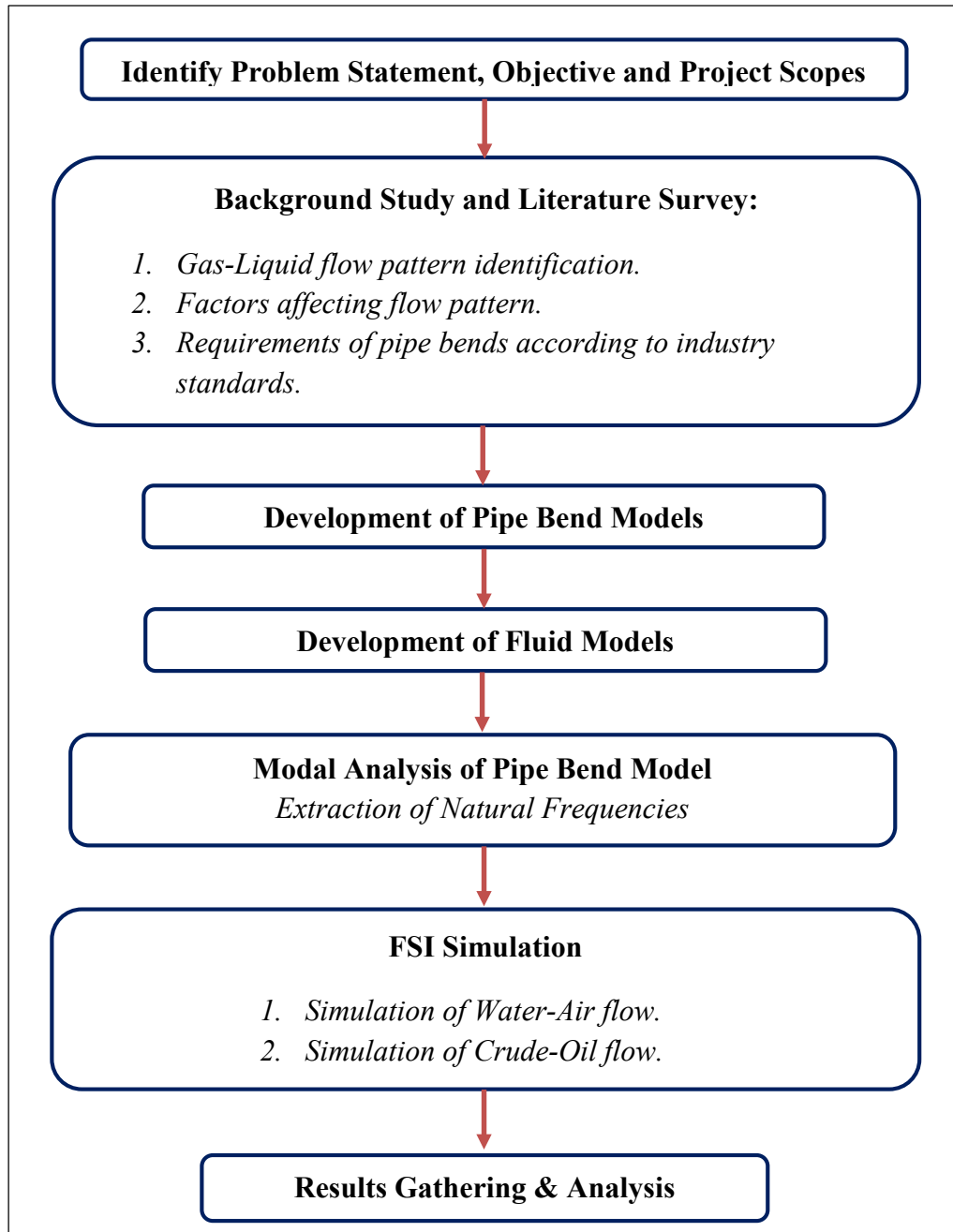


Figure 3.6: Project Flow Chart

### 3.9 Project Gantt Chart

Table 3.6: Project Gantt chart

Progress	Week number	FYPI														FYPII													
		1	2	3	4	5	6	7	8	9	10	11	12	13	14	1	2	3	4	5	6	7	8	9	10	11	12	13	14
Background study / Lit. survey				■	■	■	■	■	■	■	■	■	■	■	■														
Identify problem statement, project objectives & scopes of study			■	■		●																							
Familiarization of ANSYS software					■	■	■	■	■	■	■	■	■	■															
Development of pipe and fluid model									●																				
Simulation model development										■	■	■	■	■		■	■	■	■	■	■	■	■	■	■				
Modal Analysis Simulation													■	■	●														
Water-Air FSI Simulation (Case 1A)																■	■	■	■	■	■	●							
Water-Air FSI Simulation (Case 2A)																			■	■	■	■	●						
Crude Oil-Gas FSI Simulation (Case 1B)																				■	■	■	■	●					
Crude Oil-Gas FSI Simulation (Case 2B)																					■	■	■	■	●				
Result gathering and analysis																						■	■	■	■	■	●		
Project conclusion																								■	■	■	■	■	

● : Key Milestone

### **3.10 Tools required**

The simulation models are developed using AutoCAD. ANSYS CFX is used to simulate the two-phase flow and is coupled with ANSYS Mechanical to solve for Fluid-Structure Interaction. ANSYS CFX software is commonly employed for modeling fluid flow and heat transfer in complex geometries. It is ideally suited for both incompressible and compressible fluid-flow simulations. This software is also able to provide complete mesh flexibility including the ability to solve flow problems.

### **3.11 Concluding Remarks**

The project methodology is essential as it listed clearly all the necessary activities/stages for project completion, and explained in detail the particular project progress with respect to time. For this project, the methodology included the development of Eulerian multiphase model by referring to  $k-\omega$  SST mathematical equation. In addition, pipe bends with different upstream and downstream lengths are used to allow for slug to develop if any. The Gantt Chart was followed as per planned and by the end of the project, all simulation works and analysis have been completed.

# CHAPTER 4:

## RESULTS AND DISCUSSIONS

### 4.1 Natural Frequencies of Pipe Bend Models

The natural frequencies of the first 8 modes of the pipe structure for Case 1 and Case 2 are tabulated in Table 4.1.

**Table 4.1:** First 8 modes of Pipe Structure

Mode	Case 1	Case 2
1	6.273e-4 Hz	7.649e-4 Hz
2	3.2864 Hz	0.97033 Hz
3	3.3159 Hz	0.9952 Hz
4	8.0072 Hz	2.6634 Hz
5	18.679 Hz	12.234 Hz
6	25.32 Hz	16.75 Hz
7	448.52 Hz	107.17 Hz
8	827.51 Hz	329.41 Hz

### 4.2 Flow Patterns

The flow patterns for the free-surface model of the two-phase flow at time = 10s for Case 1A, Case 1B, Case 2A and Case 2B are as shown from Figure 4.1 to Figure 4.4 respectively.

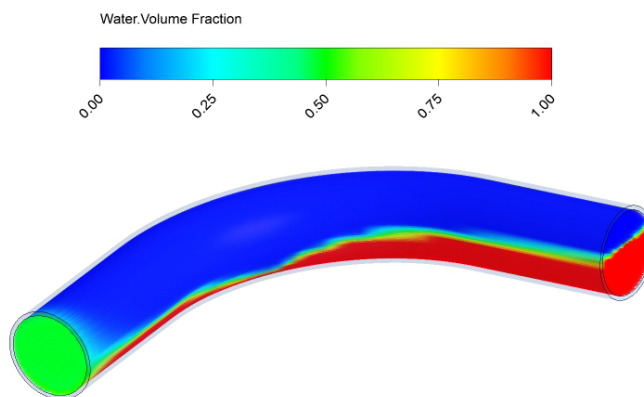


Figure 4.1: Water Volume Fraction Rendering (Case 1A)

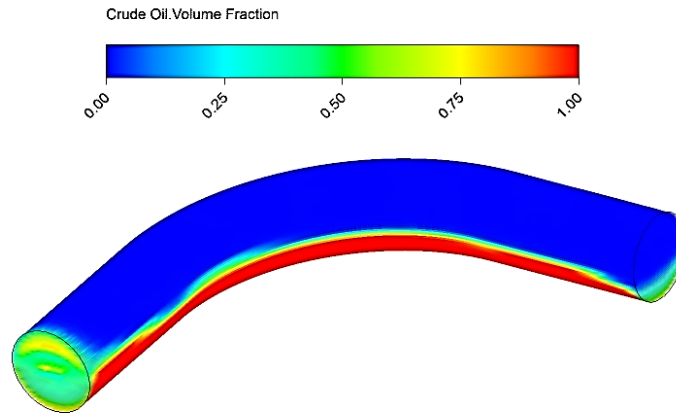


Figure 4.2: Crude Oil Volume Fraction Rendering (Case 1B)

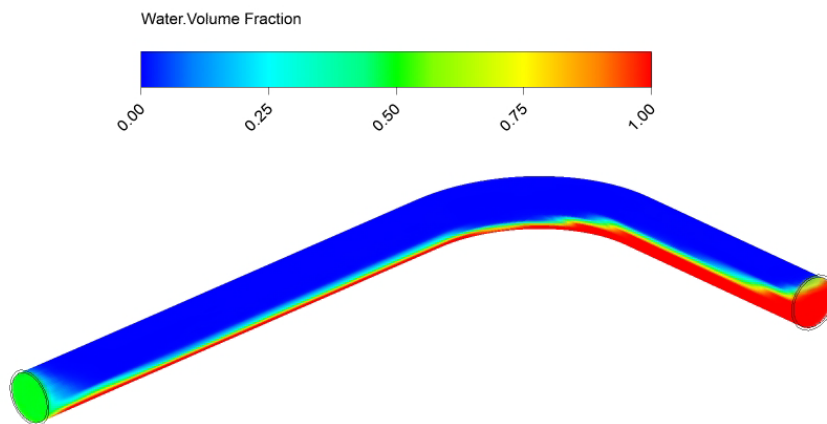


Figure 4.3: Water Volume Fraction Rendering (Case 2A)

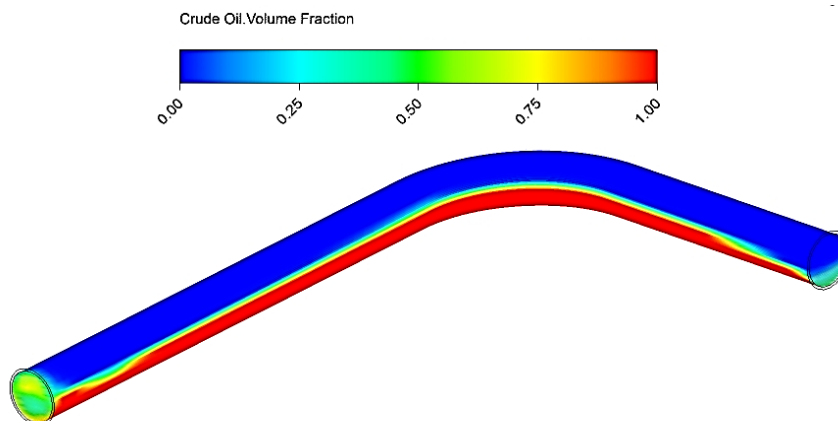


Figure 4.4: Crude Oil Volume Fraction Rendering (Case 2B)

As shown, the flows are stratified flow and no slugs have developed for both cases, although both cases have been set to parameters of slug flows according to flow regime



maps. This could be due to the slug requires a certain distance to develop. Evidently, the upstream distance of 1m of Case 2 is insufficient for the slug to develop in oil-gas flow. However, it is observed that slug almost developed at the outlet for water-air flow for both Case 1 and Case 2.

A study conducted by Chica (2014) using an M-shaped jumper with an upstream lengths of over 3.66 meter and a total length of 31.09 meter also showed absence of slug flow. Similarly, the dominant flows were stratified flows. It is therefore recommended to increase the upstream length to allow for slugs to develop. However it is difficult to predict the length.

### 4.3 Flow-Induced Vibration

As a pre-screening, a contour plot is generated to show the location of the pipe bend that is most subjected to displacement, which implies a vibration. This is illustrated in Figure 4.5.

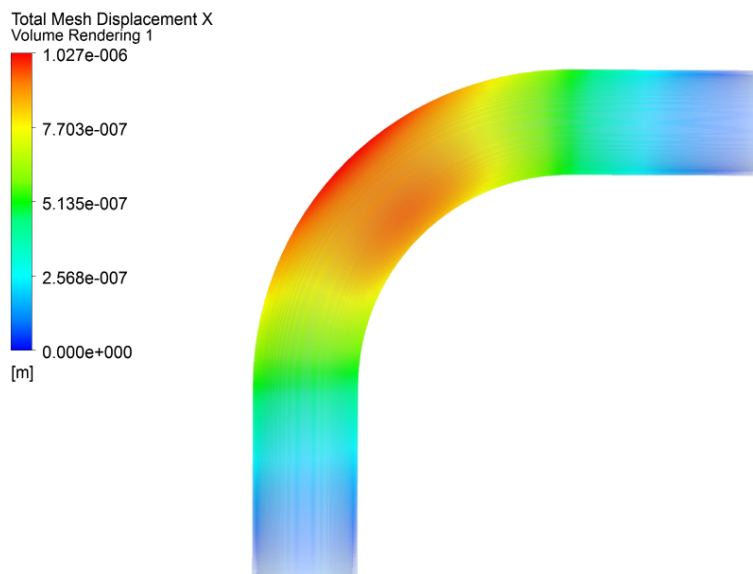


Figure 4.5: Contour Plot of Displacement of the Pipe Bend.

It is therefore justified that bends are the locations most subjected to displacement and therefore flow-induced vibrations. Charts are plotted for the fluctuations of volume fractions of liquid phase, Von Mises stress in the cross section of the bend and the displacement at a point on the bend is plotted and is shown in Figure 4.6 to Figure 4.17.

### 4.3.1 Case 1A

#### i. Volume Fraction

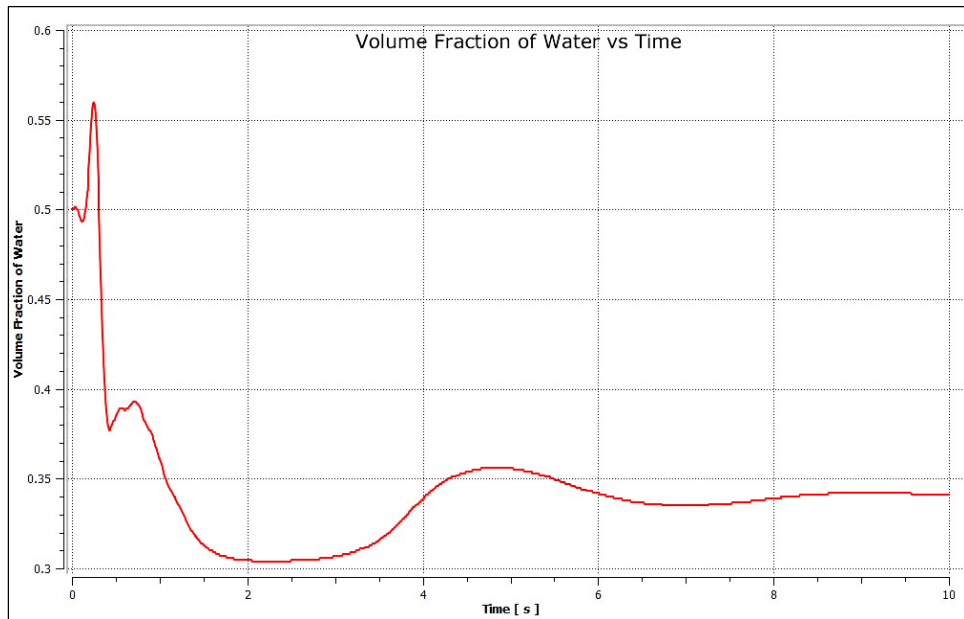


Figure 4.6(a): Volume Fraction vs Time (Case 1A)

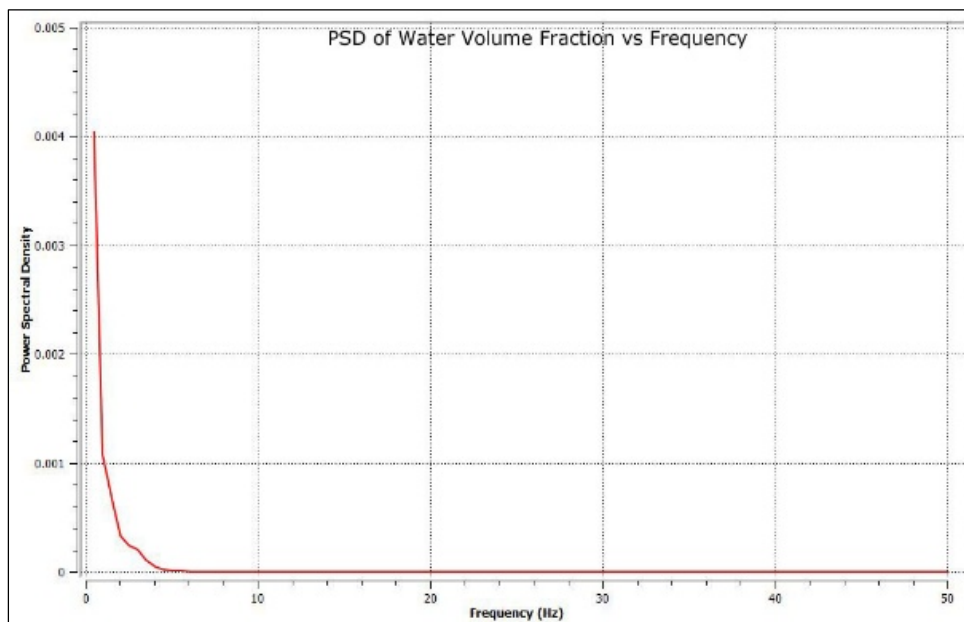


Figure 4.6(b): Volume Fraction PSD vs Frequency (Case 1A)

Figure 4.6(a) and (b) are the time domain and frequency domain of water volume fraction at the bend for Case 1A. No excitation was recorded.

ii. Von Mises Stress

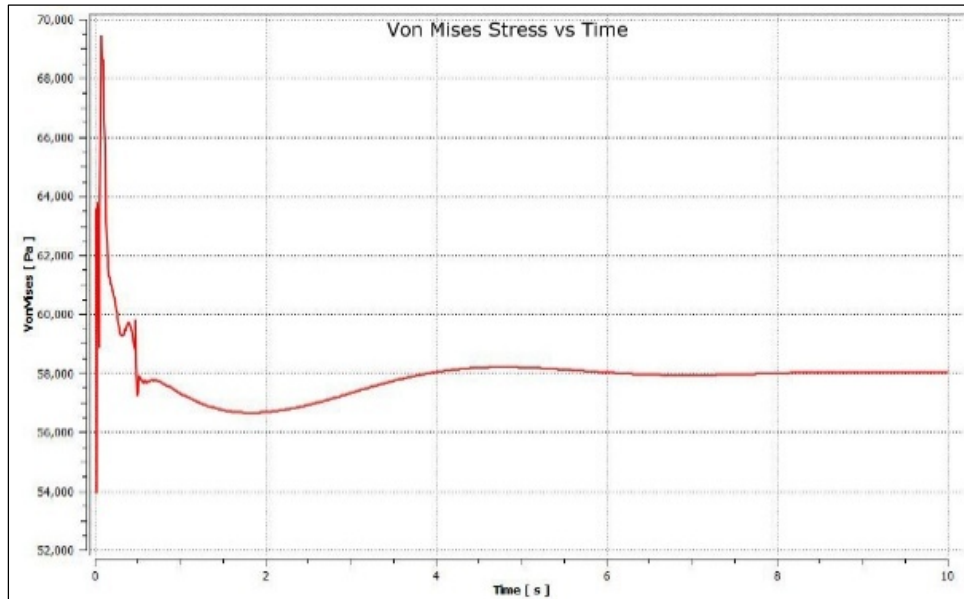


Figure 4.7(a): Von Mises Stress vs Time (Case 1A)

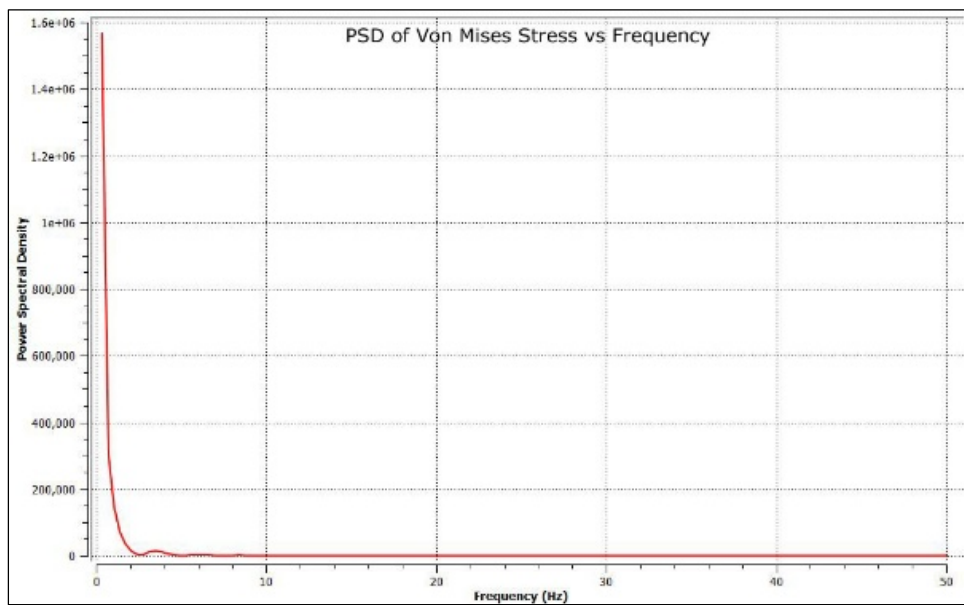


Figure 4.7(b): Von Mises Stress PSD vs Frequency (Case 1A)

Figure 4.7(a) and (b) are the time domain and frequency domain of Von Mises stress of the bend for Case 1A. No excitation was recorded.

iii. Displacement

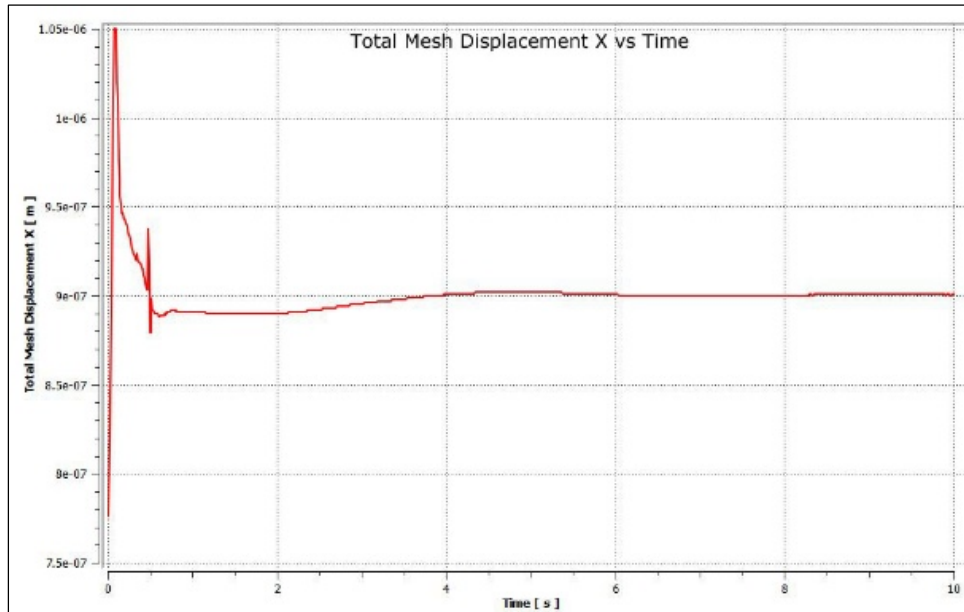


Figure 4.8(a): Displacement vs Time (Case 1A)

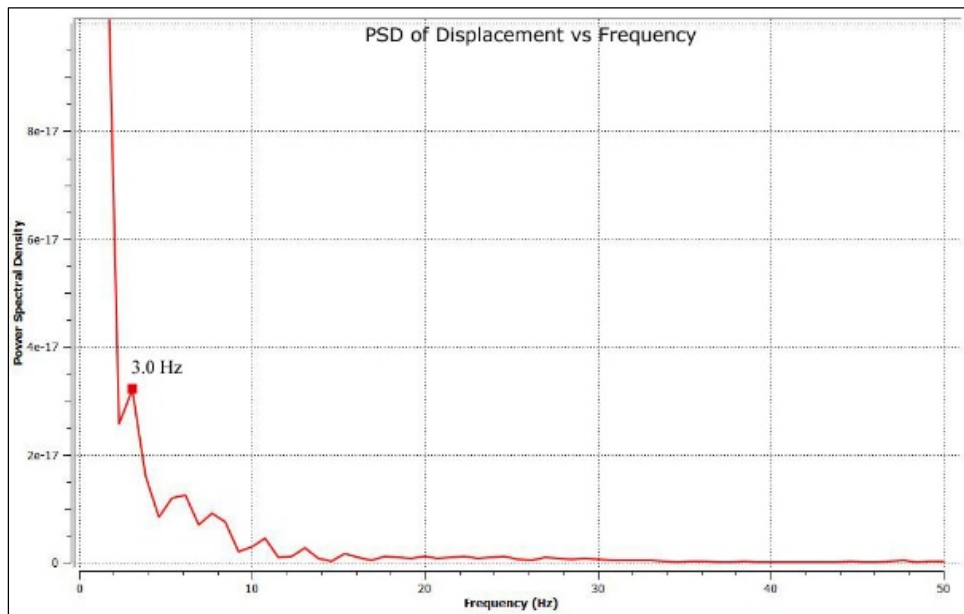


Figure 4.8(b): Displacement PSD vs Frequency (Case 1A)

Figure 4.8(a) and (b) are the time domain and frequency domain of displacement of the bend for Case 1A. An excitation frequency of **3.0 Hz** was recorded.

### 4.3.2 Case 1B

#### i. Volume Fraction

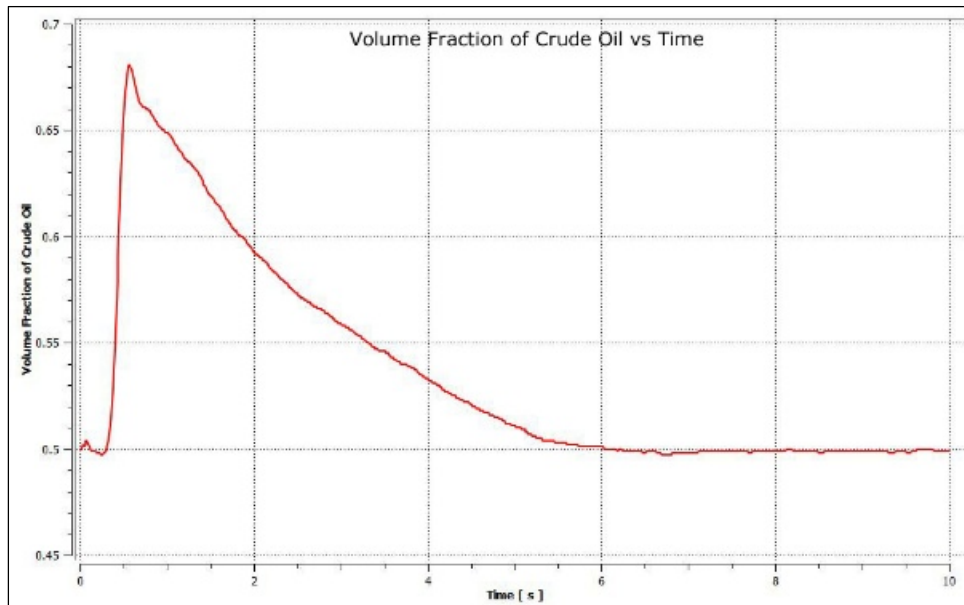


Figure 4.9(a): Volume Fraction vs Time (Case 1B)

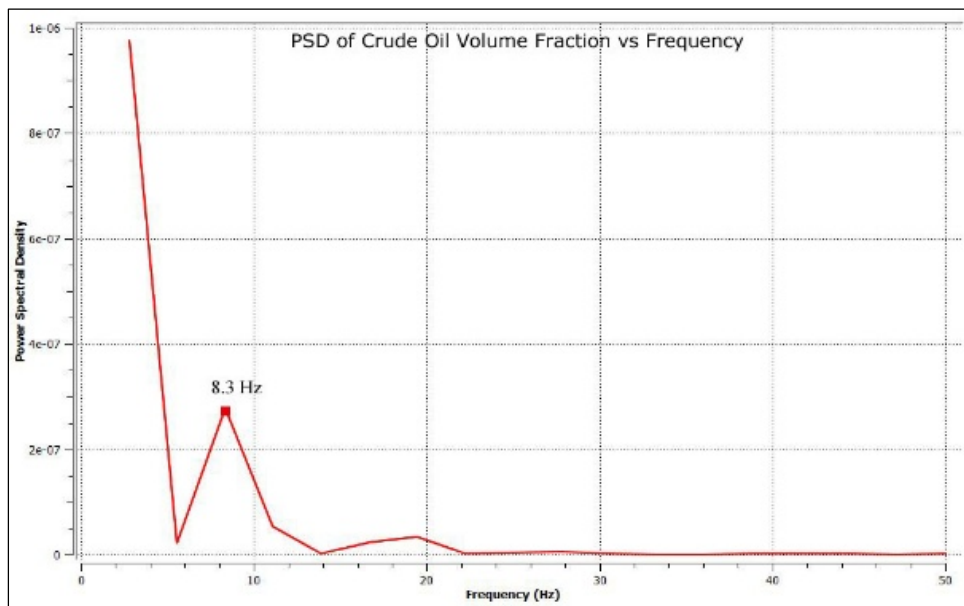


Figure 4.9(b): Volume Fraction PSD vs Frequency (Case 1B)

Figure 4.9(a) and (b) are the time domain and frequency domain of crude oil volume fraction at the bend for Case 1B. An excitation frequency of **8.3 Hz** was recorded.

ii. Von Mises Stress

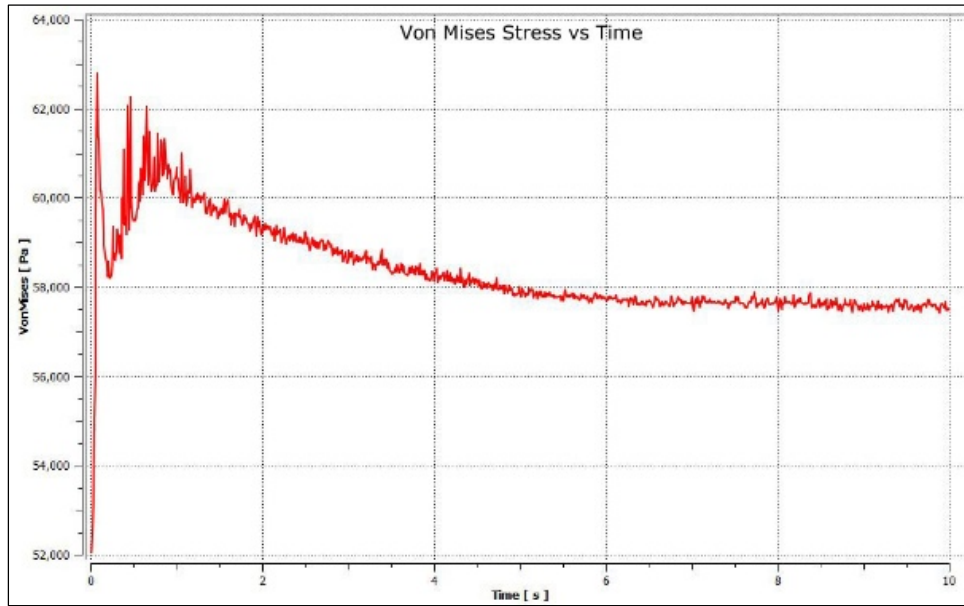


Figure 4.10(a): Von Mises Stress vs Time (Case 1B)

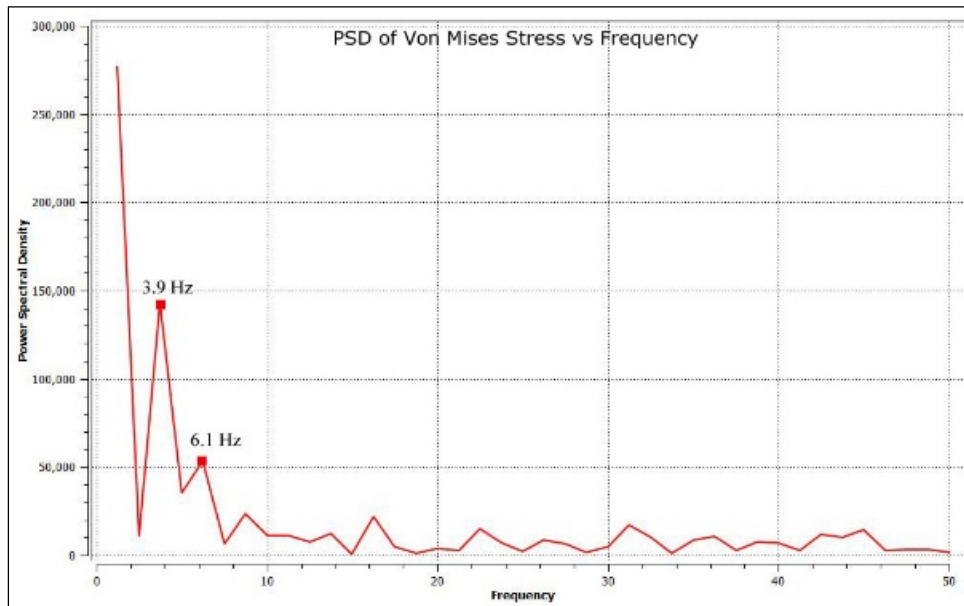


Figure 4.10(b): Von Mises Stress PSD vs Frequency (Case 1B)

Figure 4.10(a) and (b) are the time domain and frequency domain of Von Mises Stress of the bend for Case 1B. Excitation frequencies of **3.9 Hz** and **6.1 Hz** were recorded.

### iii. Displacement

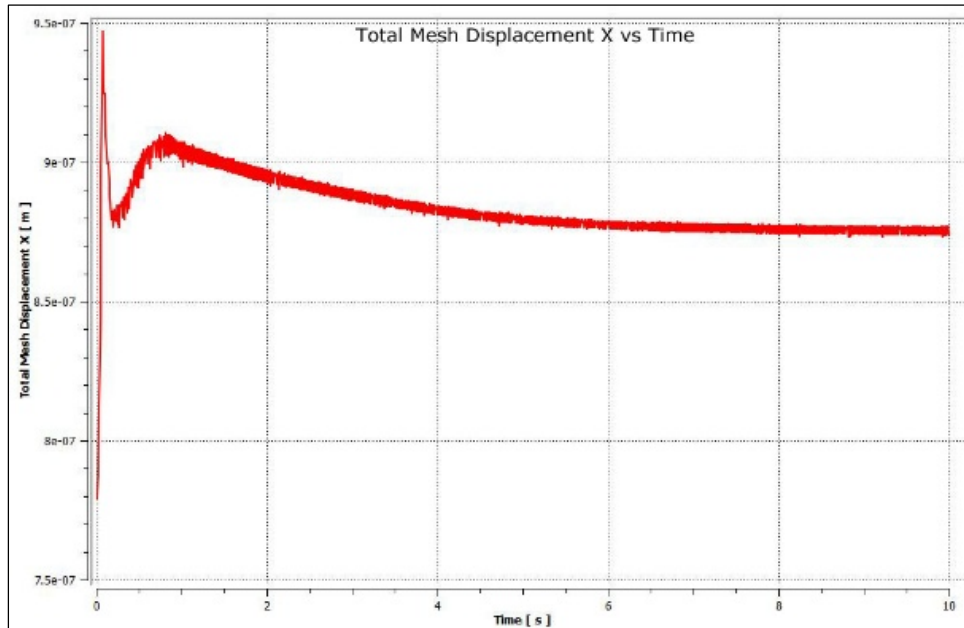


Figure 4.11(a): Displacement vs Time (Case 1B)

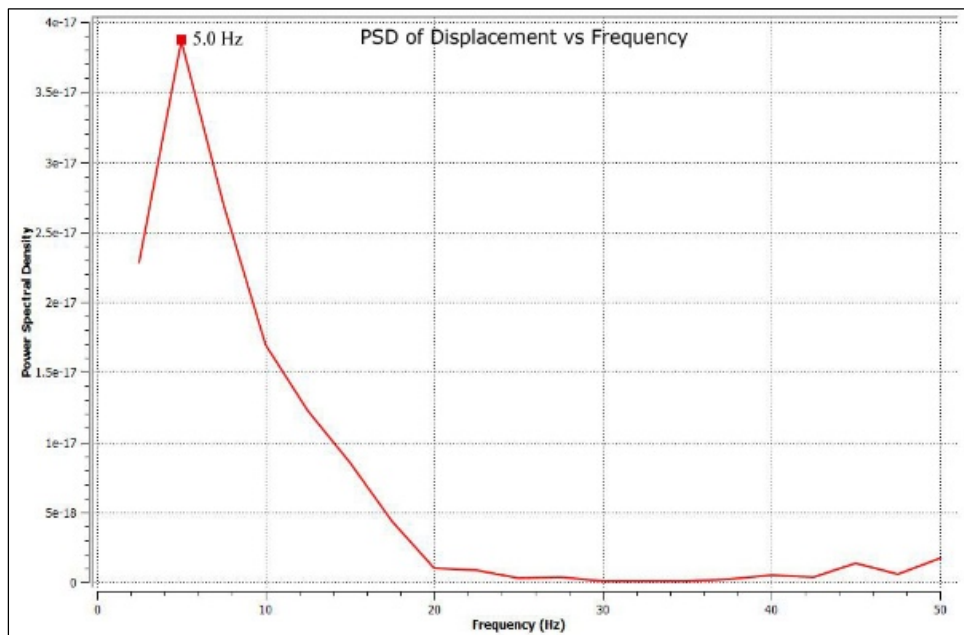


Figure 4.11(b): Displacement PSD vs Frequency (Case 1B)

Figure 4.11(a) and (b) are the time domain and frequency domain of displacement of the bend for Case 1B. An excitation frequency of **5.0 Hz** was recorded.

### 4.1.3 Case 2A

#### i. Volume Fraction

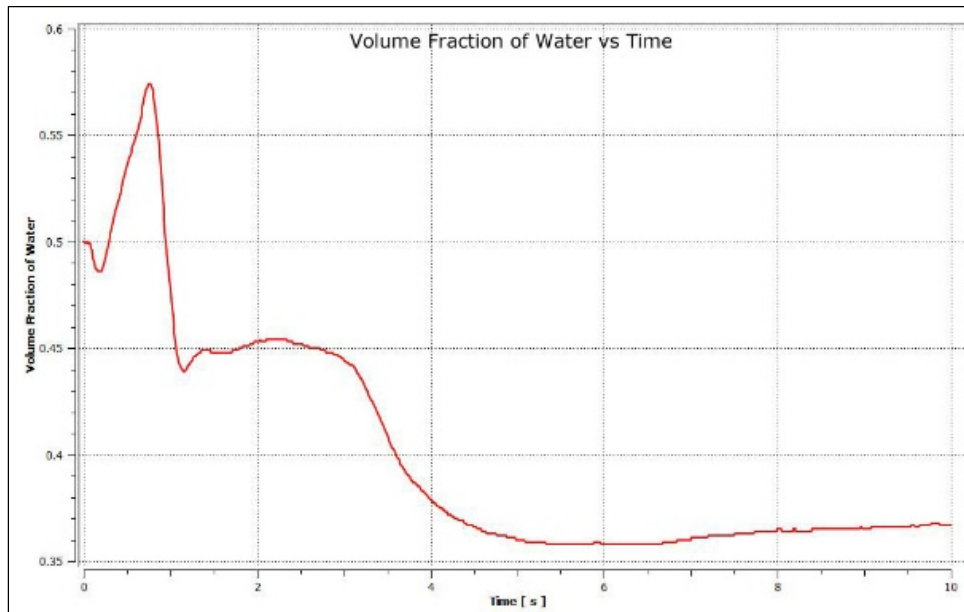


Figure 4.12(a): Volume Fraction vs Time (Case 2A)

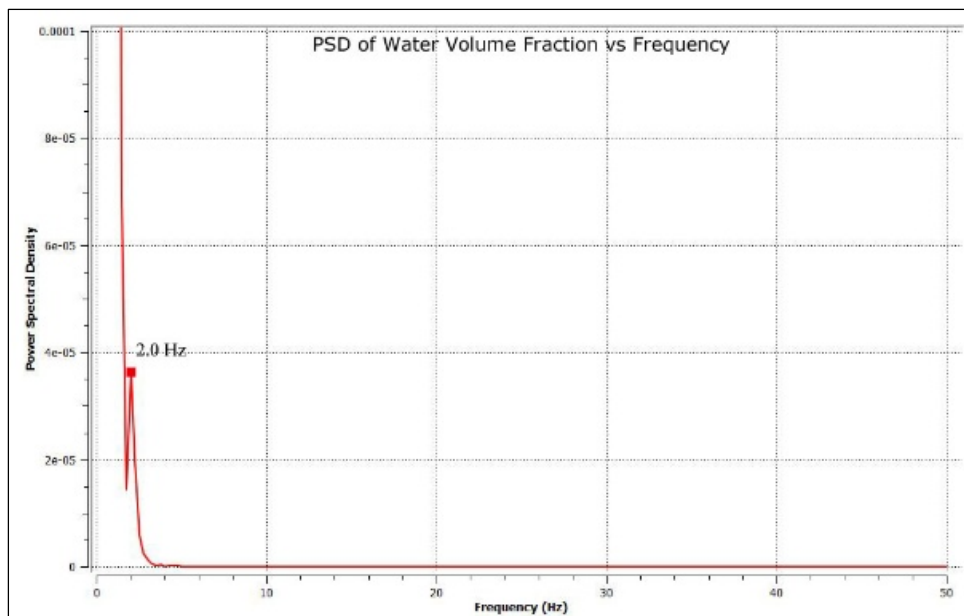


Figure 4.12(b): Volume Fraction PSD vs Frequency (Case 2A)

Figure 4.12 (a) and (b) are the time domain and frequency domain of water volume fraction at the bend for Case 2A. An excitation frequency of **2.0 Hz** was recorded.



ii. Von Mises Stress

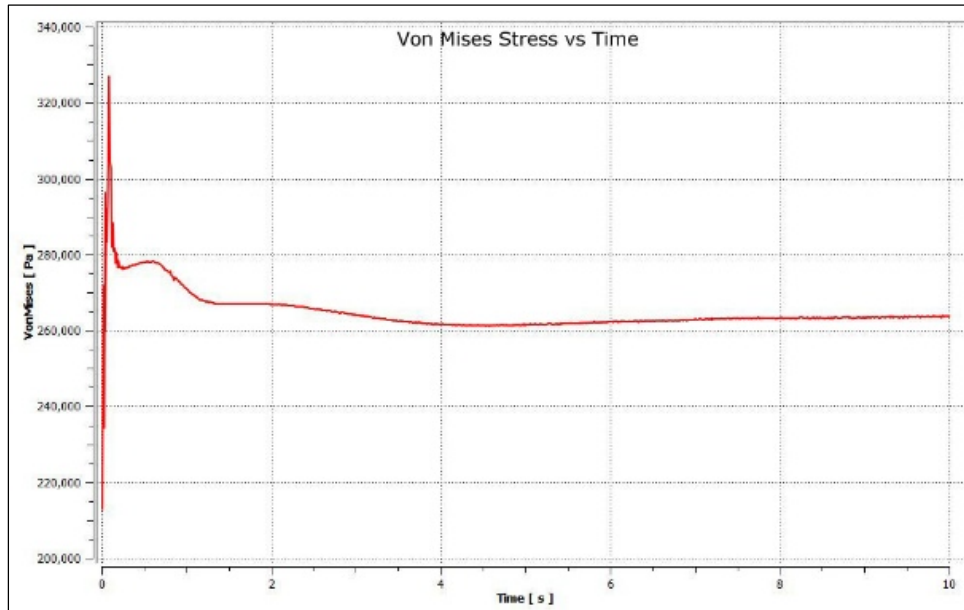


Figure 4.13(a): Von Mises Stress vs Time (Case 2A)

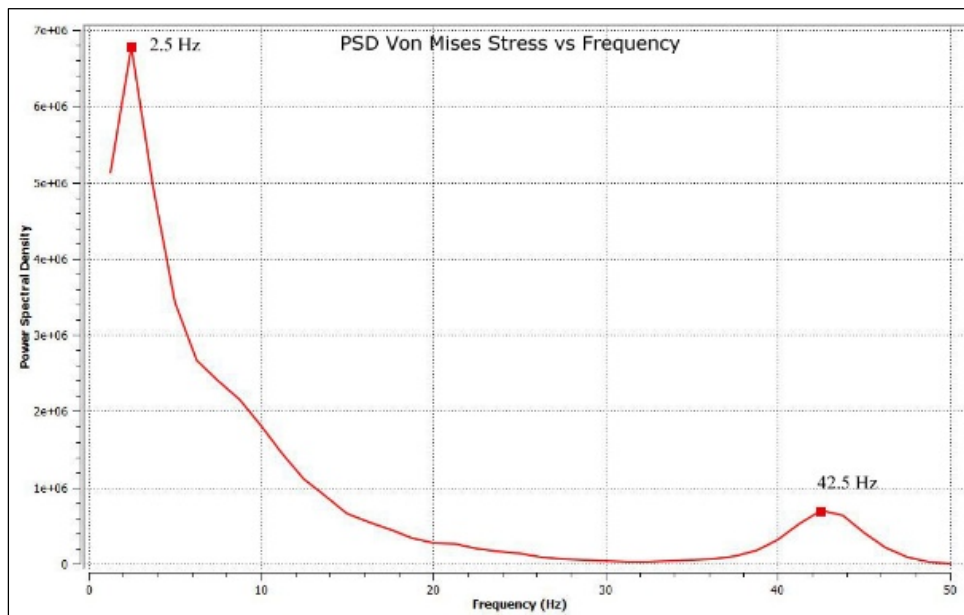


Figure 4.13(b): Von Mises Stress PSD vs Frequency (Case 2A)

Figure 4.13(a) and (b) are the time domain and frequency domain of Von Mises Stress of the bend for Case 2A. Excitation frequencies of **2.5 Hz** and **42.5 Hz** were recorded.

### iii. Displacement

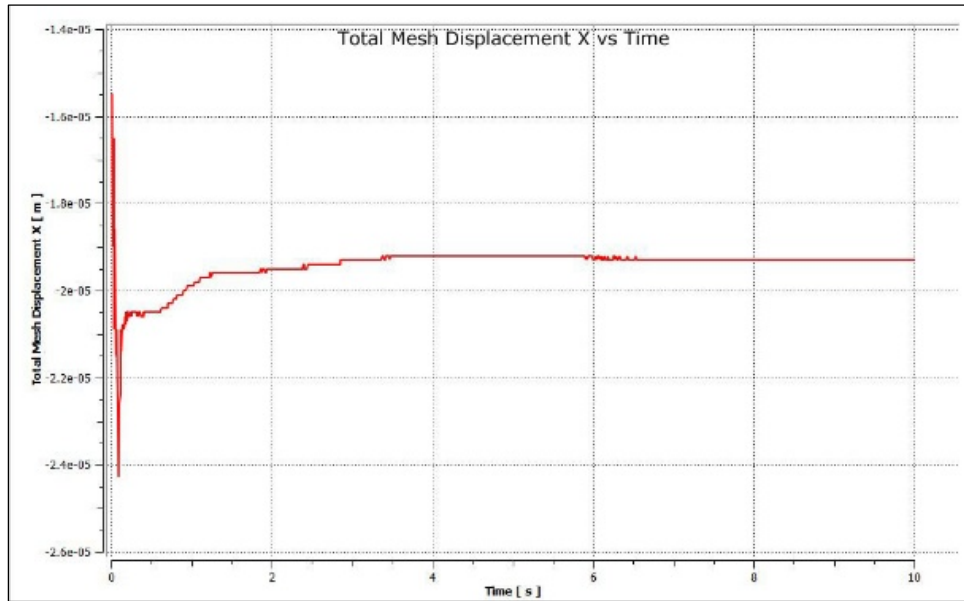


Figure 4.14(a): Displacement vs Time (Case 2A)

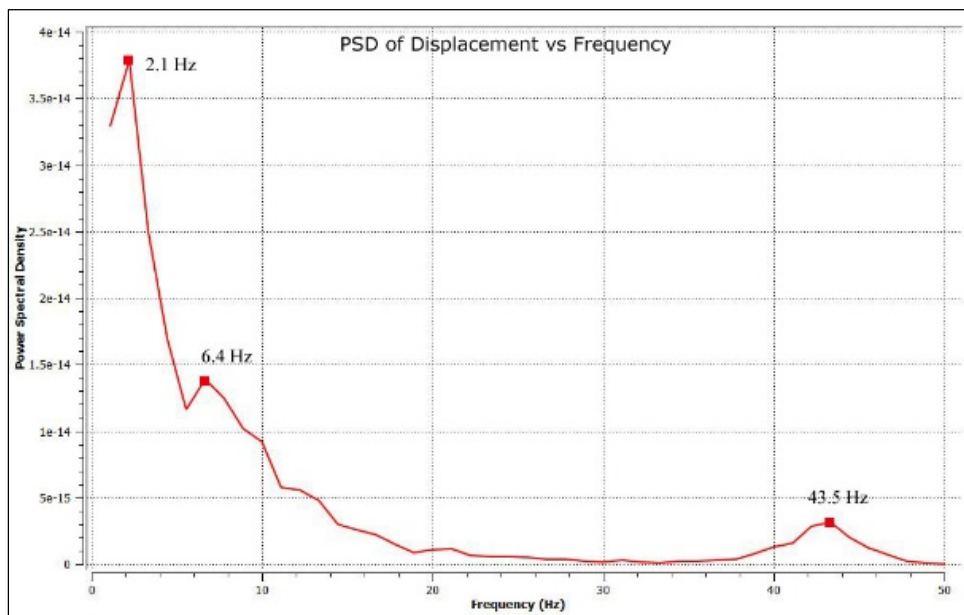


Figure 4.14(b): Displacement PSD vs Frequency (Case 2A)

Figure 4.14(a) and (b) are the time domain and frequency domain of displacement of the bend for Case 2A. Excitation frequencies of **2.1 Hz**, **6.4 Hz** and **43.5 Hz** were recorded.

#### 4.1.4 Case 2B

##### i. Volume Fraction

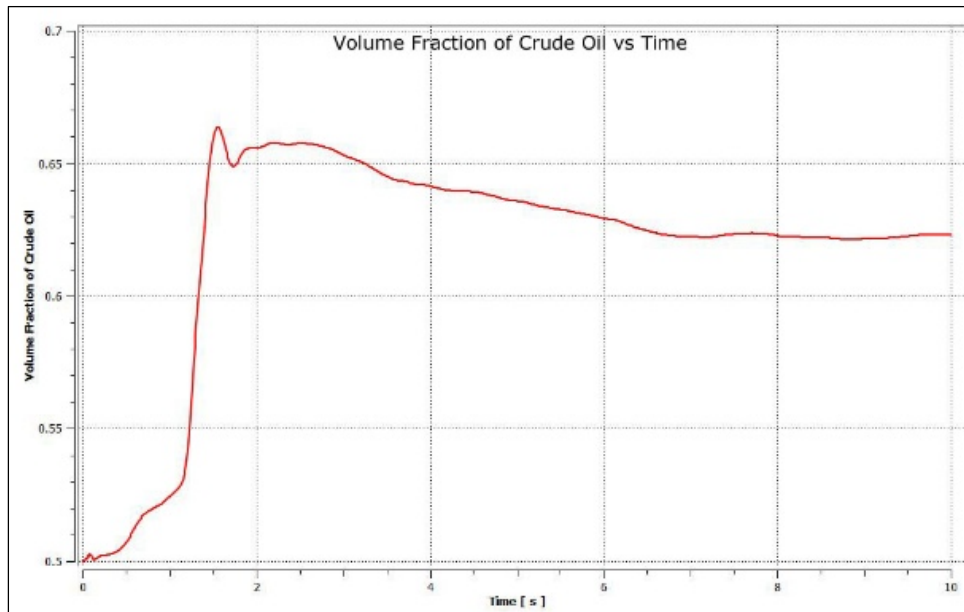


Figure 4.15(a): Volume Fraction vs Time (Case 2B)

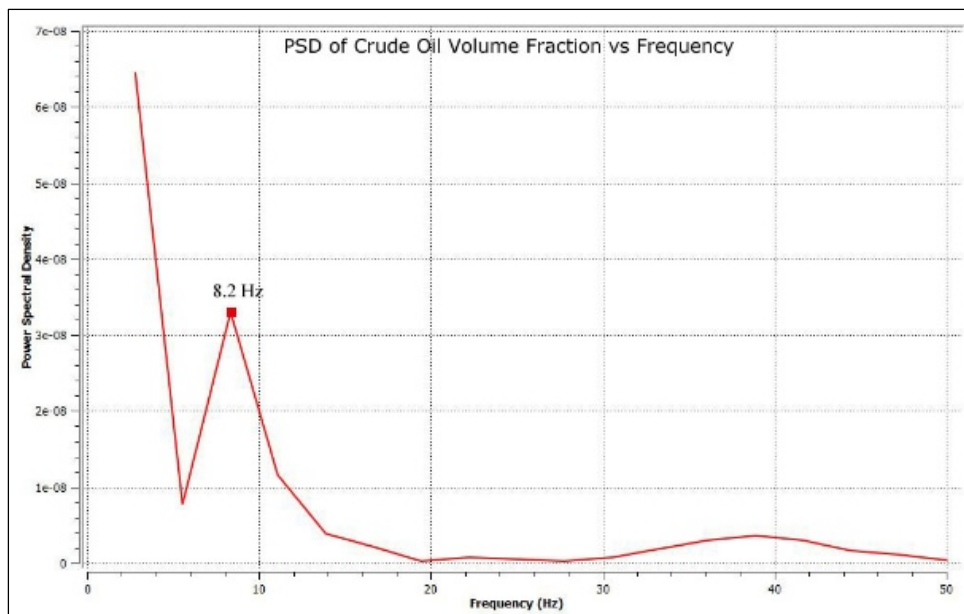


Figure 4.15(b): Volume Fraction PSD vs Frequency (Case 2B)

Figure 4.15(a) and (b) are the time domain and frequency domain of crude oil volume fraction at the bend for Case 2B. An excitation frequency of **8.2 Hz** was recorded.

ii. Von Mises Stress

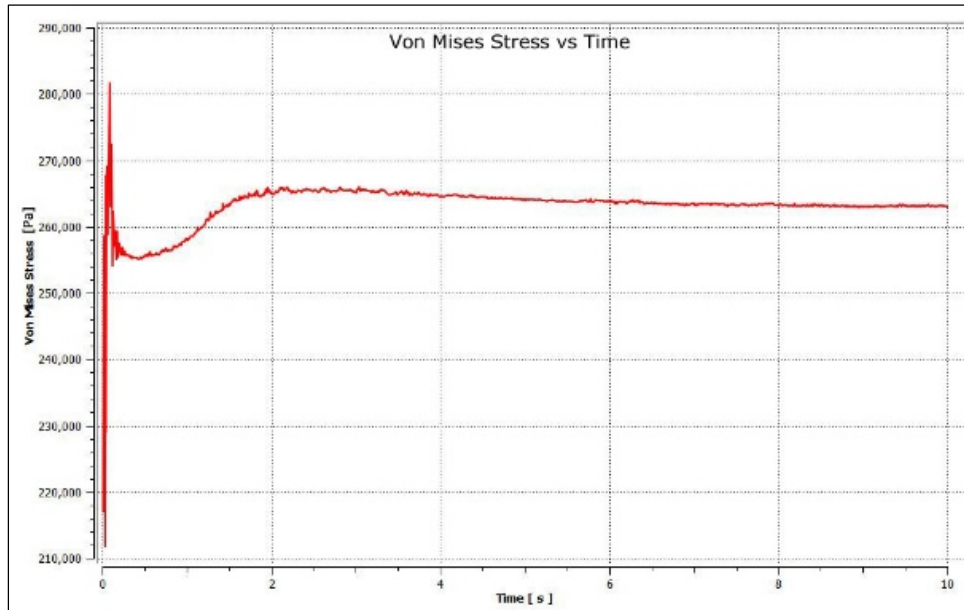


Figure 4.16(a): Von Mises Stress vs Time (Case 2B)

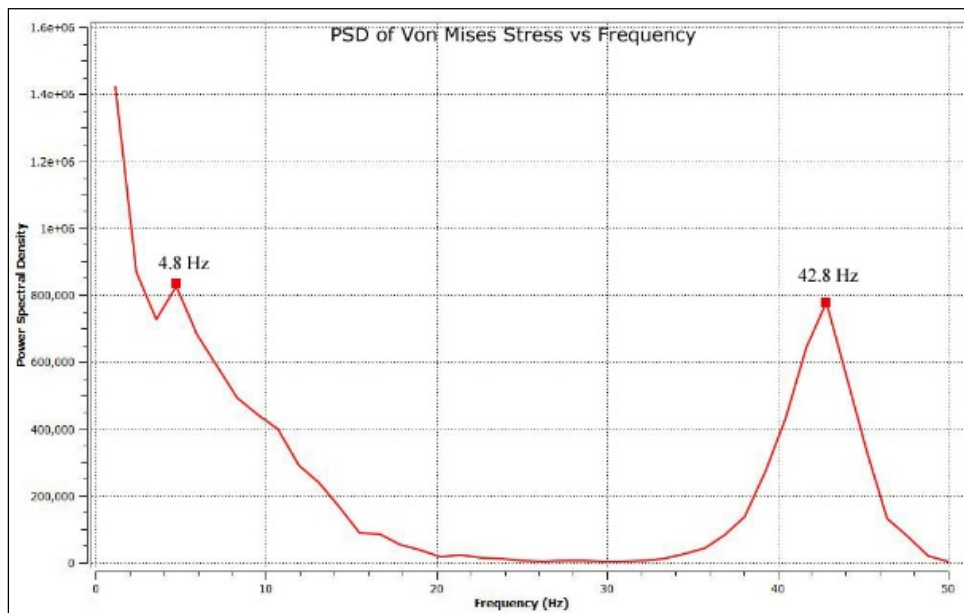


Figure 4.16(b): Von Mises Stress PSD vs Frequency (Case 2B)

Figure 4.16(a) and (b) are the time domain and frequency domain of Von Mises Stress of the bend for Case 2B. Excitation frequencies of **4.8 Hz** and **42.8 Hz** were recorded.

### iii. Displacement

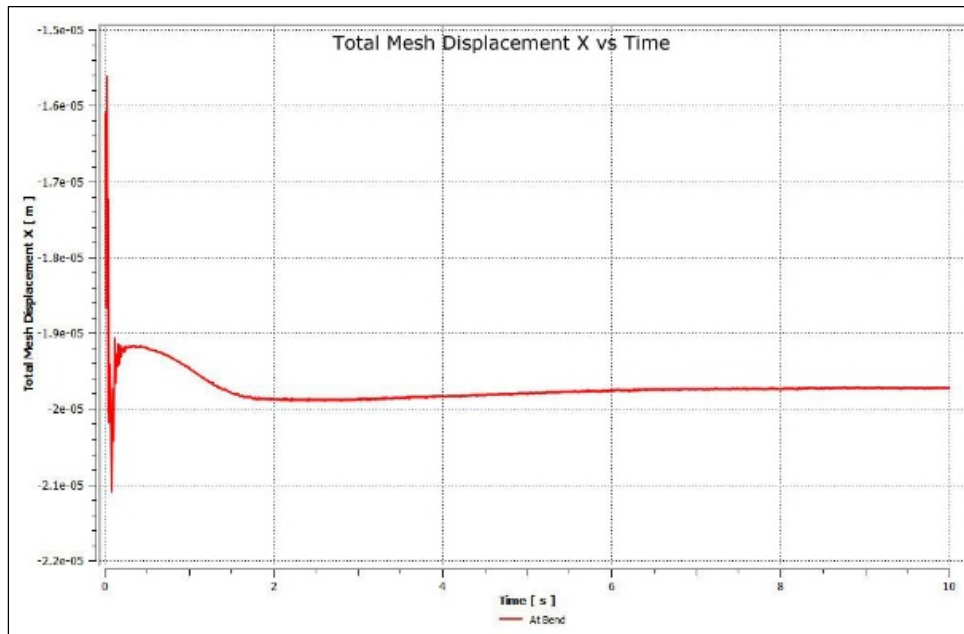


Figure 4.17(a): Displacement vs Time (Case 2B)

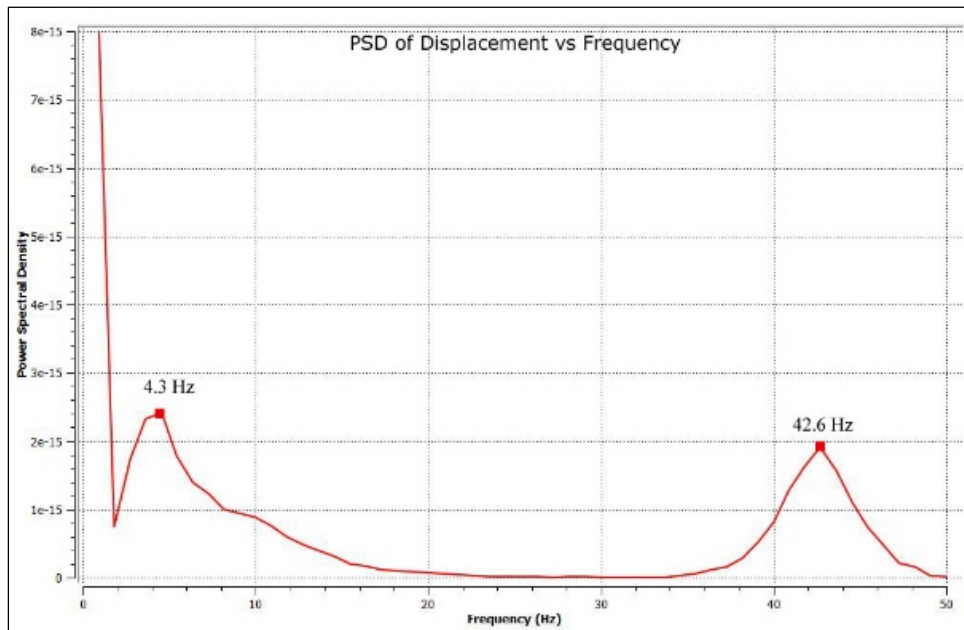



Figure 4.17(b): Displacement PSD vs Frequency (Case 2B)

Figure 4.17 (a) and (b) are the time domain and frequency domain of displacement at the bend for Case 2B. Excitation frequencies of 4.2 Hz and 42.6 Hz were recorded.

#### 4.1.5 Vibration Risk Assessment

Table 4.2: Power Spectral Density Frequency of all Cases in Comparison with Natural Frequencies

Power Spectral Density	Volume Fraction		Von Mises Stress		Displacement	
	Case 1	Case 2	Case 1	Case 2	Case 1	Case 2
Case A (Water & Air)	-	2.0 Hz	-	<b>2.5 Hz</b>	<b>3.0 Hz</b>	<b>2.1 Hz</b>
	-	-	-	42.5 Hz	-	6.4 Hz
	N/A					42.5 Hz
Case B (Oil&Gas)	<b>8.3 Hz</b>	8.2 Hz	<b>3.9 Hz</b>	4.8 Hz	5.0 Hz	4.3 Hz
	-	-	6.1 Hz	42.8 Hz	-	42.6 Hz

 Moderate Risk


 High Risk

Table 5 summarizes the dominant excitation frequency for the Power Spectral Density analysis that is Fast Fourier transformed from time domain. Yellow indicates that the excitation frequency falls between  $\pm 10 - 20\%$  of the natural frequencies (moderate risk) while red indicates that the excitation frequency falls within  $\pm 10\%$  (high risk) of natural frequencies.

## CHAPTER 5:

### CONCLUSION AND RECOMMENDATIONS

This thesis presented the fluid-structure interaction between an internally flowing two-phase flow using water & air and crude oil & gas as the medium in a pipe bend. A screening methodology monitoring changes in volume fraction in the fluid domain, and Von Mises Stress and displacement in the pipe bend was used. The results presented in this paper are limited to an internal diameter of 5cm of steel pipe with varying upstream and downstream length. It was observed that slugs hardly formed in the flow. As discussed in 4.1, a similar study by Chica (2014) using an M-shaped jumper with an upstream lengths of over 3.66 meter and a total length of 31.09 meter also showed absence of slug flow. Similarly, the dominant flows were stratified flows. It is therefore recommended to increase the upstream length to allow for slugs to develop. Otherwise, the parameters like the flow rates of each phase can be adjusted accordingly, but it would still require an appropriate parameterization of upstream lengths which is very difficult to predict due to the complexity and wide range of variables in multiphase flows.

The time domain and frequency domain of the simulations are shown from Fig. 13 to Fig. 24. These results show that there are some cases where the vibration is at high risk (Table 5), **namely 2.1 Hz for 1A, 8.3 Hz for Case 1B, and 2.5 Hz for Case 2A**. These frequencies must be avoided to avoid resonance such as the case for Tacoma Bridge collapse incident.

Vibrations are not to be taken lightly especially in flow assurance field in transporting precious hydrocarbons. Any failure in piping systems or leakage could lead to millions dollars of losses. However, vibrations are not the only problems to flow assurance. Other key problems to oil & gas industry flow assurance includes the formation of hydrates, wax, slugs, scales that could lead to corrosion and put the pipeline material integrity to risk.

## REFERENCES

1. ANSYS CFX Solver Theory Guide (2011), 14th release, ANSYS Inc., Canonsburg, Pennsylvania.
2. Bakker, A. (2006). Lecture 14 - Multiphase Flows. Applied Computational Fluid Dynamics. Retrieved from [www.bakker.org](http://www.bakker.org).
3. Brennen, C. E. (2005). Fundamentals of Multiphase Flows. California Institute of Technology. ISBN 052184040.
4. Chica, L. (2012). Fluid Structure Interaction Analysis of Two-Phase Flow in an M-shaped Jumper. Star Global Conference 2012. University of Houston, Houston, United States.
5. Chica, L. (2014). FSI Study of Internal Multiphase Flow in Subsea Piping Components. (Unpublished Master's Thesis). University of Houston, Houston, United States.
6. Crawford, N.M., Cunningham, G. & Spence, S.W.T (2007). An experimental investigation into the pressure drop for turbulent flow in 90° elbow bends. Proc Inst Mech Eng Part E: J Process Mech Eng;221(2):77e88.
7. Energy Institute, (2008). Guidelines for the avoidance of vibration induced fatigue failure in process pipework. London: Energy Institute.
8. Horgue, P., Augier, F., and Quintard, M., & Prat, M., (2012). A suitable parametrization to simulate slug flows with the Volume-Of-Fluid Method. (2012) Comptes Rendus Mécanique, vol. 340 (n° 6). pp. 411-419. ISSN1631-0721.
9. Khan, S. (2012). Flow Regime Map for Two-Phase Flow. Retrieved from <http://excelcalculations.blogspot.com/2012/02/flow-regime-map.html>
10. Mazumder, Q.H. (2012). CFD Analysis of the Effect of Elbow Radius on Pressure Drop in Multiphase Flow. University of Michigan-Flint, USA



11. Sekoda, K., Sato, Y. & Kariya, S. (1969). Horizontal Two-Phase Air-Water Flow Characteristics In the Disturbed Region due to a 90-degree Bend. *Japan Society Mechanical Engineering*, vol.35, no. 289, pp. 2227-2333.
12. Thorley, A.R.D. (2004). *Fluid Transients in Pipeline Systems: Second Edition*. Professional Engineering Publishing Limited, UK. ISBN 1-86058-405-5.
13. Vallee, C., Hohne, H., Prasser, H.M. & Suhnel, T. (2007). *Experimental Investigation and CFD Simulation of Horizontal Stratified Two-phase Flow Phenomena*. Forschungszentrum Rossendorf e. V., Dresden, Germany.
14. Wiggert, D. C., & Tijsseling, A. S. (2001). Fluid transients and fluid-structure interaction in flexible liquid-filled piping. *Applied Mechanics Reviews*, 54(5), 455. doi: 10.1115/1.1404122.

## APPENDIX

### Multiphase Flow Regime Spreadsheet

	A	B	C	D	E
1	<b>Flow Regime Calculator</b>				
2	<a href="http://excelcalculations.blogspot.com">http://excelcalculations.blogspot.com</a>				
3	The flow maps are digitized from Shell DEP 31.22.05.11				
4					
5	<b>Parameters</b>				
6		Gas	Water	Oil	
7	Mass Flow Rate (kg hr <sup>-1</sup> )	50	7000	0	
8	Density (kg m <sup>-3</sup> )	1.185	997	800	
9	Pipe ID (m)	0.05			
10					
11	<b>Calculations</b>				
12	Oil Volumetric Flow (m <sup>3</sup> hr <sup>-1</sup> )	0			
13	Water Volumetric Flow (m <sup>3</sup> hr <sup>-1</sup> )	7.021063			
14	Gas Volumetric Flow (m <sup>3</sup> hr <sup>-1</sup> )	42.19409			
15	Gas Superficial Velocity (m s <sup>-1</sup> )	5.972271			
16	Liquid Superficial Velocity (m s <sup>-1</sup> )	0.993781			
17	Water Weight Fraction	1			
18	Oil Weight Fraction	0			
19	Liquid Mixture Density (kg m <sup>-3</sup> )	997			
20	Gas Froude No (FrG)	0.294164			
21	Liquid Froude No (FrL)	1.419807			
22	Water weight fraction	0.992908			
23	Oil weight fraction	0			
24	Gas weight fraction	0.007092			
25	Mixture Density (kg m <sup>-3</sup> )	143.2486			
26	Mixture Velocity (m s <sup>-1</sup> )	6.966052			

Figure A1: Flow Regime Calculator

(Retrieved from <http://excelcalculations.blogspot.com/2012/02/flow-regime-map.html>)

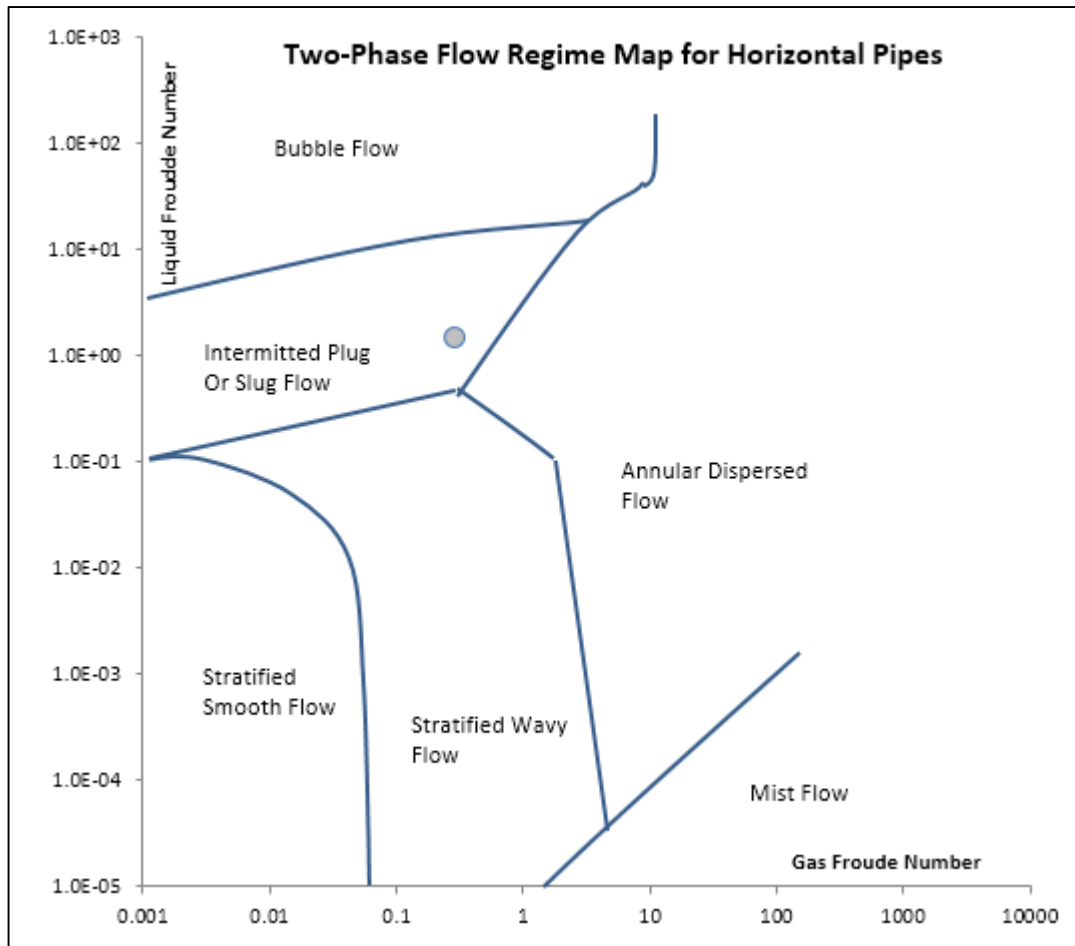


Figure A2: Digitized Two-Phase Flow Regime Map for Horizontal Pipes  
 (Retrieved from <http://excelcalculations.blogspot.com/2012/02/flow-regime-map.html>)